

Entanglement harvesting from conformal vacuums between two Unruh-DeWitt detectors moving along null paths

Subhajit Barman,^{1,*} Dipankar Barman,^{1,†} and Bibhas Ranjan Majhi^{1,‡}

¹*Department of Physics, Indian Institute of Technology Guwahati, Guwahati 781039, Assam, India*

(Dated: December 3, 2021)

It is well-known that the $(1+1)$ dimensional Schwarzschild and spatially flat FLRW spacetimes are conformally flat. This work examines entanglement harvesting from the conformal field vacuums in these spacetimes between two Unruh-DeWitt detectors, moving along outgoing null trajectories. In $(1+1)$ dimensional Schwarzschild spacetime, we considered the Boulware and Unruh vacuums for our investigations. We also considered the momentum-space representation of Green's functions and linear couplings between the field and the detectors to estimate the concurrence and the mutual information corresponding to specific field mode frequency. In this analysis, one observes that while entanglement harvesting is possible in $(1+1)$ dimensional Schwarzschild and $(1+3)$ dimensional de Sitter spacetimes, it is not possible in the $(1+1)$ dimensional de Sitter background for the same set of parameters when the detectors move along the same outgoing null trajectory. The qualitative results from the Boulware and the Unruh vacuums are alike. Furthermore, we observed that the concurrence depends on the distance d between the two null paths of the detectors in a periodic manner. In $(1+1)$ dimensional Schwarzschild and $(1+3)$ dimensional de Sitter backgrounds one obtains specific periodic points in d for which concurrence vanishes. While in $(1+1)$ dimensional de Sitter spacetime, one gets specific periodic regions in d with vanishing concurrence. We also observe that the mutual information does not depend on d in $(1+1)$ dimensional Schwarzschild and de Sitter spacetimes but periodically depends on it in $(1+3)$ dimensional de Sitter background.

PACS numbers: 04.62.+v, 04.60.Pp

I. INTRODUCTION

The fascinating phenomenon of quantum entanglement has garnered significant interest in the scenarios of relativistic particles in flat and curved spacetimes [1–18]. Studying the dynamics of entangled particles in flat and curved spacetimes [9, 19–21] has presented many enthralling perspectives. Another interesting facet is the possibility of entanglement extraction [1, 6, 22–28] from the quantum field into atoms or other suitable systems interacting with the field, which is known as entanglement harvesting. The prospect of utilizing this harvested entanglement in quantum information-related purposes [29–31] to solidify experimental verification of many theoretical predictions has made the harvesting a desirable arena to venture further.

Reznik solidified the possibility of harvesting entanglement from the vacuum of the background quantum field in [1, 25] where he recognized entanglement extraction in a system of two anti-parallelly accelerated two-level atomic detectors. Reznik's work signifies the role of the quantum field vacuum in entanglement extraction as one observes entanglement harvesting between two causally disconnected accelerated detectors with no possibility of classical correlation. His works and the subsequent works [7, 32–41] usually deal with a system composed of two de-

tectors that interact with the background field and are in an initial uncorrelated state. One can perceive any entanglement harvested between the two detectors by checking whether the partial transposition of the final system reduced density matrix has negative eigenvalues [42, 43]. We mention that one realizes this reduced density matrix as the system's final density matrix with the field degrees of freedom traced out. This formulation was further improved in [44–49], where the authors considered proper time ordering into the picture. It resulted in the introduction of the Feynman propagator rather than the Wightman function in some places of the estimated eigenvalues. We mention that the entanglement harvesting condition and the measure of the harvested entanglement depends on the background geometry [32–34, 49–51], boundary conditions [15, 50, 52], the two detectors' trajectories [6, 49, 53], etc.

Recently, entanglement harvesting in black hole spacetimes [26, 47, 49, 54] has gained much interest. In this context, which vacuum to choose in these spacetimes to formulate quantum field theory and obtain the Green's functions corresponding to observers in different trajectories has a general notion [49]. Namely, in an $(1+1)$ dimensional Schwarzschild background, these are the *Boulware*, *Unruh*, and *Hartle-Hawking vacuums* [49]. They denote conformal vacuums corresponding to different coordinate choices in the background spacetime, as all $(1+1)$ dimensional spacetimes are conformally flat [55, 56]. We mention that the spatially flat *Friedman-Lemaître-Robertson-Walker* (FLRW) metric is also conformally flat. One should also note that nontrivial findings for entanglement harvesting is closely related to semi-classical particle cre-

*Electronic address: subhajit.b@iitg.ac.in

†Electronic address: dipankar1998@iitg.ac.in

‡Electronic address: bibhas.majhi@iitg.ac.in

ation. However, in a $(1+1)$ dimensional Schwarzschild background, a static observer does not see the Boulware vacuum to be particle creating. Likewise, with static detectors, one obtains entanglement harvesting related observations from the Boulware vacuum that are similar to the flat spacetime [49]. Furthermore, in [57], it was shown that a radially in-falling detector in a time-like trajectory observes the Boulware vacuum to be thermal. These freely-falling detectors also keep nontrivial entanglement harvesting profiles from the Boulware vacuum, as was pointed out in [49]. Subsequently, in [58, 59], one also observes the thermal nature of the Boulware vacuum and that of the conformal vacuum in the FLRW spacetime, with detectors infalling in null-like trajectories. These facts motivated us to study entanglement-related phenomena with detectors in null paths in the $(1+1)$ dimensional Schwarzschild and FLRW spacetimes. In particular, we shall investigate the entanglement harvesting from the above-mentioned conformal vacuums in these backgrounds. This consideration of null trajectories for detectors in black hole spacetimes is interesting from the point of view that it may shed light on the entanglement harvested between light-like particles emitted from astrophysical bodies along null paths. In this regard, we mention that these are situations related to the Hawking effect, as originally, Hawking, in his pioneering work [60] elucidated the black hole evaporation in terms of field modes in ingoing and outgoing null trajectories. Thus our consideration of entanglement harvesting along null trajectories may open up directions to provide new insights towards the understanding of the black hole information loss paradox and also remains relevant from the cosmological point of view.

As we have already stated, in this work, we study the entanglement harvesting conditions with Unruh-DeWitt detectors in null trajectories in the background of $(1+1)$ -dimensional Schwarzschild black holes and the FLRW spacetime. The Unruh-DeWitt detectors conceptualized to understand the Unruh effect [61–63], are point-like two-level hypothetical detectors. In particular, we have considered estimating the entanglement harvesting condition in the de Sitter era of the FLRW universe. We also mention that we obtain the entanglement harvesting condition for each specific field mode frequency. We observe that entanglement harvesting is indeed possible from the conformal vacuums in $(1+1)$ dimensional Schwarzschild, $(1+1)$ and $(1+3)$ dimensional FLRW spacetimes with two detectors in outgoing null paths. In all these cases, the concurrence, which measures the harvested entanglement, peaks at a particular field mode frequency. Furthermore, the interesting phenomenon is that this concurrence is, in all these cases, periodically dependent on the distance d between different outgoing null paths of the two detectors. It also gives rise to specific periodic distance points in $(1+1)$ dimensional Schwarzschild, $(1+3)$ dimensional de Sitter, and certain distance regions in $(1+1)$ dimensional de Sitter spacetimes where the concurrence vanishes. Thus providing the notion of the so-

called entanglement shadow points and shadow regions [54], from where one cannot harvest entanglement. However, unlike [54] where the entanglement shadow region appears near the black hole event horizon, in our case, these regions are periodic in the distance d . On the other hand, we observe that the mutual information in $(1+1)$ dimensional Schwarzschild and de Sitter spacetimes are independent of this distance d between the null paths of the two detectors. However, in $(1+3)$ dimensional de Sitter spacetime, the mutual information is dependent on d . We also observe that it is periodic with the distance d between different outgoing null paths of the two detectors.

We organize this paper in the following way. In Sec. II we start with a brief overview of the model set-up for entanglement harvesting with two two-level point-like atomic detectors interacting with the background massless real scalar field through monopole couplings. This section elucidates the entanglement harvesting condition, the measure of the harvested entanglement (the concurrence), and the total correlation (the mutual information). In Sec. III we illuminate the importance of conformal vacuum in curved spacetimes to formulate quantum field theory and briefly discuss the construction of these vacuums in FLRW and $(1+1)$ dimensional Schwarzschild spacetimes. Subsequently, in Sec. V we consider a massless conformally invariant scalar field in these spacetimes and construct the necessary Green's functions for observers in null trajectories. In Sec. VI we study the entanglement harvesting condition from the conformal vacuum in the spacetimes as mentioned earlier and also study the entanglement measure concurrence. In the following section VII we investigate the mutual information in the considered spacetimes. We conclude this work in Sec. VIII with a discussion of our findings.

II. MODEL SET-UP

In this section, we will briefly discuss the model set up for entanglement harvesting, emphasizing the necessary notations and symbols of the different system parameters. This model was introduced initially in [44–46], which keeps into consideration the necessary time ordering in the construction of the Green's functions.

In this model set-up, one considers two point-like two-level Unruh-DeWitt detectors, each carried by a distinct observer. One of these observers is Alice denoted by A , and another one is Bob denoted by B . We denote the detector states as $|E_n^j\rangle$, with the symbols delineating the n^{th} state of j^{th} detector, i.e., we have $j = A, B$ and $n = 0, 1$. We also consider these states to be non degenerate so that $E_1^j \neq E_0^j$, and the difference $\Delta E^j = E_1^j - E_0^j > 0$ signifies the transition frequency. Furthermore, we consider a massless, minimally coupled real scalar field $\Phi(X)$ interacting with these detectors through monopole couplings $m^j(\tau_j)$. One can express

the corresponding interaction action as

$$S_{int} = \int_{-\infty}^{\infty} \left[c_A \kappa_A(\tau_A) m^A(\tau_A) \Phi(X_A(\tau_A)) d\tau_A + c_B \kappa_B(\tau_B) m^B(\tau_B) \Phi(X_B(\tau_B)) d\tau_B \right], \quad (1)$$

where, c_j , $\kappa_j(\tau_j)$, and τ_j respectively denote the couplings between the individual detectors and the scalar field, the switching functions, and the individual detec-

tor proper times. We consider the initial detector field state in the asymptotic past to be $|in\rangle = |0\rangle|E_0^A\rangle|E_0^B\rangle$, where $|0\rangle$ denotes the field's ground state. Then the final detector field state in asymptotic future will be $|out\rangle = T\{e^{iS_{int}}|in\rangle\}$, where T signifies time ordering. One can get the explicit expression of this final state by treating the coupling constants c_j perturbatively. In this way and by tracing out the final field degrees of freedoms one obtains the final detector density matrix in the basis of $\{|E_1^A\rangle|E_1^B\rangle, |E_1^A\rangle|E_0^B\rangle, |E_0^A\rangle|E_1^B\rangle, |E_0^A\rangle|E_0^B\rangle\}$ as

$$\rho_{AB} = \begin{bmatrix} 0 & 0 & 0 & c_A c_B \varepsilon \\ 0 & c_A^2 P_A & c_A c_B P_{AB} & c_A^2 W_A^{(N)} + c_A c_B W_A^{(S)} \\ 0 & c_A c_B P_{AB}^* & c_B^2 P_B & c_B^2 W_B^{(N)} + c_A c_B W_B^{(S)} \\ c_A c_B \varepsilon^* & c_A^2 W_A^{(N)*} + c_A c_B W_A^{(S)*} & c_B^2 W_B^{(N)*} + c_A c_B W_B^{(S)*} & 1 - (c_A^2 P_A + c_B^2 P_B) \end{bmatrix} + \mathcal{O}(c^4), \quad (2)$$

where, P_j , ε , $W_j^{(N)}$, and $W_j^{(S)}$ are explicitly expressed as

$$P_j = |\langle E_1^j | m_j(0) | E_0^j \rangle|^2 \mathcal{I}_j$$

$$\varepsilon = \langle E_1^B | m_B(0) | E_0^B \rangle \langle E_1^A | m_A(0) | E_0^A \rangle \mathcal{I}_\varepsilon$$

$$P_{AB} = \langle E_1^A | m_A(0) | E_0^A \rangle \langle E_1^B | m_B(0) | E_0^B \rangle^\dagger \mathcal{I}_{AB}$$

$$W_j^{(N)} = \langle E_1^j | m_j(0) | E_0^j \rangle \left[\left(\langle E_1^j | m_j(0) | E_1^j \rangle - \langle E_0^j | m_j(0) | E_0^j \rangle \right) \mathcal{I}_{j,1}^{(N)} - i \langle E_0^j | m_j(0) | E_0^j \rangle \mathcal{I}_{j,2}^{(N)} \right]$$

$$W_j^{(S)} = -i \langle E_1^j | m_j(0) | E_0^j \rangle \langle E_0^{j'} | m_{j'}(0) | E_0^{j'} \rangle \mathcal{I}_j^{(S)}, \quad (3)$$

where $j' \neq j$ and the quantities \mathcal{I} 's are given by

$$\mathcal{I}_j = \int_{-\infty}^{\infty} d\tau_j' \int_{-\infty}^{\infty} d\tau_j e^{-i\Delta E^j(\tau_j' - \tau_j)} G_W(X_j', X_j),$$

$$\mathcal{I}_\varepsilon = -i \int_{-\infty}^{\infty} d\tau_B' \int_{-\infty}^{\infty} d\tau_A e^{i(\Delta E^B \tau_B' + \Delta E^A \tau_A)} G_F(X_B', X_A),$$

$$\mathcal{I}_{AB} = \int_{-\infty}^{\infty} d\tau_B' \int_{-\infty}^{\infty} d\tau_A e^{i(\Delta E^A \tau_A - \Delta E^B \tau_B')} G_W(X_B', X_A),$$

$$\mathcal{I}_{j,1}^{(N)} = \int_{-\infty}^{\infty} d\tau_j' \int_{-\infty}^{\infty} d\tau_j e^{i\Delta E^j \tau_j} \theta(\tau_j' - \tau_j) G_W(X_j', X_j),$$

$$\mathcal{I}_{j,2}^{(N)} = \int_{-\infty}^{\infty} d\tau_j' \int_{-\infty}^{\infty} d\tau_j e^{i\Delta E^j \tau_j} G_R(X_j, X_j'),$$

$$\mathcal{I}_j^{(S)} = \int_{-\infty}^{\infty} d\tau_j' \int_{-\infty}^{\infty} d\tau_j e^{i\Delta E^j \tau_j} G_R(X_j, X_j'). \quad (4)$$

Here we have considered $\kappa_j(\tau_j) = 1$, i.e., the detectors are eternally interacting with the field. The expressions of the quantities $G_W(X_j, X_{j'})$, $G_F(X_j, X_{j'})$, and $G_R(X_j, X_{j'})$; which respectively denote the positive frequency Wightman function with $X_j > X_{j'}$, the Feynman propagator, and the retarded Green's function; are [44]

$$\begin{aligned} G_W(X_j, X_{j'}) &\equiv \langle 0_M | \Phi(X_j) \Phi(X_{j'}) | 0_M \rangle, \\ G_F(X_j, X_{j'}) &\equiv -i \langle 0_M | T \{ \Phi(X_j) \Phi(X_{j'}) \} | 0_M \rangle, \\ G_R(X_j, X_{j'}) &\equiv i \theta(t - t') \langle 0_M | [\Phi(X_{j'}), \Phi(X_j)] | 0_M \rangle. \end{aligned} \quad (5)$$

We refer the readers to [44] for a complete analysis.

From the general study [42, 43] of bipartite systems, it is observed that one must have a negative eigenvalue of the partial transposition of the reduced detector density matrix for entanglement harvesting. Here, with the reduced density matrix (2) this condition results in

$$P_A P_B < |\varepsilon|^2. \quad (6)$$

Moreover, in terms of the integrals (4) this condition (6) takes the form [44, 46]

$$\mathcal{I}_A \mathcal{I}_B < |\mathcal{I}_\varepsilon|^2. \quad (7)$$

We mention that the Feynman propagator and the Wightman functions are related

among themselves [44] as $iG_F(X_j, X_{j'}) = G_W(X_j, X_{j'}) + iG_R(X_{j'}, X_j) = G_W(X_j, X_{j'}) + \theta(T' - T) \{G_W(X_{j'}, X_j) - G_W(X_j, X_{j'})\}$, which can be used to further simplify the expression of the integral \mathcal{I}_ε of (4) as

$$\mathcal{I}_\varepsilon = - \int_{-\infty}^{\infty} d\tau_B \int_{-\infty}^{\infty} d\tau_A e^{i(\Delta E^B \tau_B + \Delta E^A \tau_A)} \times [G_W(X_B, X_A) + \theta(T_A - T_B) \{G_W(X_A, X_B) - G_W(X_B, X_A)\}]. \quad (8)$$

This particular expression is advantageous because all of the integrals \mathcal{I}_A , \mathcal{I}_B and \mathcal{I}_ε , imperative for the verification of the entanglement harvesting condition (7), are now expressed in terms of the Wightman functions. Furthermore writing the \mathcal{I}_ε in this form also enables one to identify the separate contributions with or without the considered time ordering. Note that condition (7) is constructed at the order c^2 in perturbation series. Later on our whole analysis will be done at this order.

After the condition for entanglement harvesting (7) is met, one is prompted to quantify its measures. The common entanglement measures are negativity and concurrence [64–67]. Negativity signifies the upper bound of the distillable entanglement, and one obtains it from the sum of all negative eigenvalues of the partial transpose of ρ_{AB} . Concurrence $\mathcal{C}(\rho_{AB})$ is another convenient entanglement measure [20, 44, 46], which enables one to find the entanglement of formation [44, 46, 68–70]. In the two qubits system, the concurrence is given by [44]

$$\begin{aligned} \mathcal{C}(\rho_{AB}) &= \max \left[0, 2c^2 \left(|\varepsilon| - \sqrt{P_A P_B} \right) + \mathcal{O}(c^4) \right] \\ &\approx \max \left[0, 2c^2 |\langle E_1^B | m_B(0) | E_0^B \rangle| |\langle E_1^A | m_A(0) | E_0^A \rangle| \right. \\ &\quad \left. \times \left(|\mathcal{I}_\varepsilon| - \sqrt{\mathcal{I}_A \mathcal{I}_B} \right) \right], \end{aligned} \quad (9)$$

where, we have assumed $c_A = c_B = c$, i.e., both detectors have equal couplings with the scalar field. Now the quantities $|\langle E_1^j | m_j(0) | E_0^j \rangle|$ are obtained from the detectors' internal structure; the spacetime and background scalar fields do not contribute in them. Then to understand the effects of the trajectories and the spacetime in the harvested entanglement, we shall only study the relevant quantity

$$\mathcal{C}_\mathcal{I} = \left(|\mathcal{I}_\varepsilon| - \sqrt{\mathcal{I}_A \mathcal{I}_B} \right) \quad (10)$$

with the intention of studying the concurrence. Note in the symmetric case $\mathcal{I}_A = \mathcal{I}_B$, this quantity becomes $\mathcal{C}_\mathcal{I} = (|\mathcal{I}_\varepsilon| - \mathcal{I}_j)$, see [44, 46].

Another measure of correlation is mutual information \mathcal{M} , which signifies the total of classical and quantum correlations, defined as

$$\mathcal{M}(\rho_{AB}) \equiv S(\rho_A) + S(\rho_B) - S(\rho_{AB}), \quad (11)$$

where, $\rho_A \equiv \text{Tr}_B(\rho_{AB})$ and $\rho_B \equiv \text{Tr}_A(\rho_{AB})$ are the reduced density matrices corresponding to the detectors A and B , and $S(\rho) \equiv -\text{Tr}(\rho \ln \rho)$ signifies the von Neumann entropy corresponding to the density matrix ρ . With the density matrix (2), and considering equal couplings between the two detectors and field, one can express the mutual information [71] of (11) as

$$\begin{aligned} \mathcal{M}(\rho_{AB}) &= c^2 [P_+ \ln P_+ + P_- \ln P_- - P_A \ln P_A \\ &\quad - P_B \ln P_B] + \mathcal{O}(c^4), \end{aligned} \quad (12)$$

where, the quantities P_\pm are given by

$$P_\pm = \frac{1}{2} \left[P_A + P_B \pm \sqrt{(P_A - P_B)^2 + 4|P_{AB}|^2} \right]. \quad (13)$$

In a system, if the mutual information is non-zero but the concurrence vanishes, then the correlation is considered classical. Consequently, we shall look into both concurrence and mutual information to understand the nature of the correlation between the two detectors.

III. CONFORMAL VACUUM FOR TWO DIMENSIONAL SCHWARZSCHILD BLACK HOLE AND FLRW UNIVERSE

In this section, we are going to discuss the conformal vacuum associated with a $(1+1)$ dimensional Schwarzschild and *Friedman-Lemaître-Robertson-Walker* (FLRW) spacetime. Although the concept is elaborated in literature [55, 56] in great detail, here we shall provide a brief outline of the essential elements necessary for our study. Introducing a conformally invariant field in conformally flat spacetime allows one to realize flat-space-like quantum field theory in a curved background without moving to its asymptotic regions. The metric tensor corresponding to a conformally flat spacetime can be expressed as

$$g_{\mu\nu}(x) = \Omega^2 \eta_{\mu\nu}(x), \quad (14)$$

where Ω^2 is the conformal factor, and $\eta_{\mu\nu}(x)$ denotes the metric tensor in a Minkowski spacetime. In a conformally flat spacetime it is necessary to consider a massless ($m = 0$) scalar field $\Phi(x)$ to obtain a conformally invariant wave equation. In particular, this wave equation is expressed as

$$(\square - \xi R) \Phi(x) = 0, \quad (15)$$

where the operator \square in the background spacetime is given by $\square\Phi = (\sqrt{-g})^{-1/2} \partial_\mu [\sqrt{-g} g^{\mu\nu} \partial_\nu \Phi]$, R represents the Ricci scalar, and ξ the conformal coupling. In an n -dimensional spacetime this conformal coupling is of the form $\xi = (n-2)/4(n-1)$. Therefore, ξ vanishes in $(1+1)$ -dimensional spacetime and $\xi = 1/6$ for $(1+3)$ -dimensions. It is to be noted that with a further decomposition of the conformally invariant field $\Phi = \Omega^{(2-n)/2} \tilde{\Phi}$, the above wave equation reduces to that

of the flat spacetime, $\eta^{\mu\nu}\partial_\nu\partial_\mu(\bar{\Phi}) = 0$. Then one could readily find out the mode solutions \bar{u}_k of the field $\bar{\Phi}$, which are plane wave like. In terms of these mode functions one may express the scalar field $\Phi(x)$ as

$$\Phi(x) = \Omega^{(2-n)/2}(x) \sum_k [\hat{a}_k \bar{u}_k(x) + \hat{a}_k^\dagger \bar{u}_k^*(x)] . \quad (16)$$

Here the annihilation operator \hat{a}_k annihilates the conformal vacuum $|0\rangle$, i.e., $\hat{a}_k|0\rangle = 0$. This brief summary highlights the advantages of considering a conformally coupled scalar field in a conformally flat spacetime to observe the effects of quantum field theory. It should be noted that all $(1+1)$ dimensional spacetimes and the spatially flat FLRW spacetime are conformally flat. In our subsequent analysis we shall briefly discuss the conformal nature of Schwarzschild and FLRW spacetimes.

A. Two dimensional Schwarzschild spacetime

In this part, we are going to elucidate on the Schwarzschild spacetime briefly. In particular, we shall concentrate on the $(1+1)$ dimensional representation of it. There are a few necessary reasons behind considering the $(1+1)$ dimensional representation. In our context, the most important reason is that all $(1+1)$ dimensional spacetimes are conformally flat, as we have previously mentioned. Then one can effortlessly utilize quantum field theory in this background. For semi-classical particle production, one usually needs the understanding of wave modes in ingoing and outgoing null paths in a black hole background. This picture is efficiently understandable in an $(1+1)$ dimensional representation of a generally higher-dimensional black hole spacetime to produce the thermal behavior of the Hawking effect. This outcome also becomes relevant in our scenario, as Entanglement harvesting is closely related to particle production. The $(1+1)$ dimensional representation of the Schwarzschild solution is considered to understand the entanglement harvesting conditions with static and free-falling detectors in literature [49], which will also help us compare our results.

In fact, the $(1+1)$ dimensional Schwarzschild black hole can be considered as the solution of a two dimensional Einstein-Dilaton theory [56, 72] which is a dimensionally reduced form of higher dimensional usual Einstein's theory of gravity. In particular, in $(1+1)$ dimensions the line-element in Schwarzschild background using the Schwarzschild coordinates (t_s, r) is given by

$$ds^2 = -\left(1 - \frac{r_H}{r}\right) dt_s^2 + \left(1 - \frac{r_H}{r}\right)^{-1} dr^2 , \quad (17)$$

where, r_H represents the Schwarzschild radius. It is observed that in terms of the tortoise coordinate r_* , defined from

$$dr_* = \frac{dr}{1 - r_H/r} , \quad (18)$$

the $(1+1)$ dimensional Schwarzschild metric becomes

$$ds^2 = \left(1 - \frac{r_H}{r}\right) [-dt_s^2 + dr_*^2] . \quad (19)$$

The expression of this metric is analogous to the prescription of (14) with $\Omega^2 = (1 - r_H/r)$, which ensures that the $(1+1)$ dimensional Schwarzschild black hole spacetime is conformally flat. One can easily obtain the scalar field decomposition like (16) in this spacetime, with the wave modes now expressed in terms of t_s and r_* . In particular, the related conformal vacuum is known as the Boulware vacuum.

We mention that the conformal metric of (19) can also be represented in terms of the null coordinates $u = t_s - r_*$ and $v = t_s + r_*$, thus the Boulware modes are eligible to be represented in terms of these null coordinates. These null coordinates are related to the Kruskal coordinates as $V = 2r_H e^{v/2r_H}$ and $U = -2r_H e^{-u/2r_H}$. One may move to these Kruskal coordinates also and find the metric of Eq. (19) again to be conformally flat, but with different conformal factors. We mention that considering different sets of these coordinates one obtains different conformal vacuums corresponding to the Schwarzschild black hole spacetime. Specifically with u and v the vacuum is Boulware, with U and v the vacuum is Unruh, and U and V the vacuum is Hartle-Hawking [49, 73].

A static observer in a Schwarzschild black hole spacetime does not observe the Boulware vacuum to be filled with particles. However, a freely in-falling observer perceives the Boulware vacuum to be thermal, as was pointed out by recent studies [57]. On the other hand, entanglement related observations are highly connected to the scenarios of particle creation in a curved spacetime [49]. Therefore, we shall consider these types of relevant paths, which can observe particles in these vacua, for the observation of entanglement harvesting.

B. The FLRW spacetime

After briefly elucidating on the static black hole spacetime we now proceed to the *Friedman-Lemaître-Robertson-Walker* (FLRW) spacetime, which is an exact solution of the Einstein's field equations with positive cosmological constant. The FLRW metric was formulated to represent our universe and indicates spatial homogeneity, isotropy, and expansion. In $(1+1)$ -dimensional FLRW spacetime the line element is given by

$$ds = -dt^2 + a^2(t) dx^2 , \quad (20)$$

where $a(t)$ denotes the scale factor, which is different in different eras of the universe. In particular, in this work we shall consider the de Sitter era, where one can analytically pursue the calculations. In de Sitter era the scale factor is $a(t) = e^{t/\alpha_d}$, which describes the early expansion of the homogeneous, isotropic universe. In terms of

the conformal time η , related to the coordinate time t through $d\eta = dt/a(t)$, expressed in de Sitter background

$$\eta = -\alpha_d e^{-t/\alpha_d}, \quad (21)$$

the line element becomes

$$ds^2 = a^2(\eta)(-d\eta^2 + dx^2). \quad (22)$$

Like the (1+1) dimensional Schwarzschild spacetime here also one can observe that the background spacetime becomes conformally flat with $\Omega = a(\eta)$, and one can easily find out the scalar field decomposition like (16) with respect to the coordinates η and x .

On the other hand, in (1+3)-dimensional FLRW spacetime the line element is given by

$$\begin{aligned} ds^2 &= -dt^2 + a^2(t)|d\vec{x}|^2 \\ &= a^2(\eta)(-d\eta^2 + |d\vec{x}|^2). \end{aligned} \quad (23)$$

Here also the spacetime is conformally flat and one is eligible to decompose a conformally coupled scalar field in terms of plane wave modes. It is to be noted that, in both the (1+1) and (1+3) dimensional de Sitter spacetimes the conformal vacuums for observers with coordinates (η, \vec{x}) are perceived to be particle creating with respect to a comoving observer with coordinates (t, \vec{x}) .

In [58], it is shown that an observer in a null like trajectory also observes the conformal vacuum particle generating. We have already stated semi-classical particle creation is closely related to non-trivial findings in the entanglement harvesting conditions. In our subsequent studies we shall be discussing about the null paths in these spacetimes which are related to particle creation. Furthermore, we shall investigate the entanglement harvesting conditions in these scenarios.

IV. NULL PATHS RELATED TO PARTICLE CREATION FROM THE CONFORMAL VACUUM

Here we discuss a class of trajectories, specifically the null paths, from which an observer perceives the conformal vacuum to be particle creating. First, in a (1+1) dimensional black hole Schwarzschild spacetime Eq. (19) signifies that a radially moving object is following an outgoing null path if $u = t_s - r_*$ is constant along its trajectory. On the other hand, it is ingoing when $v = t_s + r_*$ is constant. These two coordinates are often referred to as the retarded and advanced time coordinates or the outgoing and ingoing null coordinates. In terms of the Eddington-Finkelstein (EF) coordinates (t, r) , with $t + r = t_s + r_*$ the metric (19) transforms to

$$ds^2 = -\left(1 - \frac{r_H}{r}\right)dt^2 + \frac{2r_H}{r}dt dr + \left(1 + \frac{r_H}{r}\right)dr^2. \quad (24)$$

With these EF coordinates one can find out an outgoing

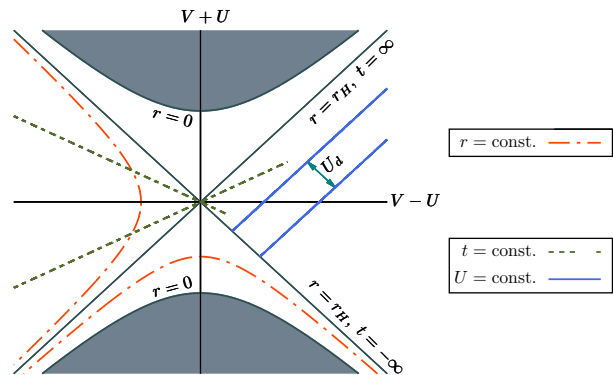


FIG. 1: Schematic representation of two detectors in outgoing null paths depicted in a Kruskal diagram. In Eddington-Finkelstein coordinates the two detectors are separated as $u_A - u_b = d$, while in Kruskal coordinates they are separated as $U_d = U_B - U_A = 2r_H(1 - e^{-d/2r_H})$, where $U_j = -2r_H e^{-u_j/2r_H}$.

null trajectory by making $ds^2 = 0$ in (24) and considering the positive solution of dr/dt , see [59], as

$$\frac{dt}{dr} = \frac{r/r_H + 1}{r/r_H - 1}, \quad (25)$$

which gives the path to be

$$t = r + 2r_H \ln \left[\frac{r}{r_H} - 1 \right] + d. \quad (26)$$

Here d is a constant parameter arriving as an integration constant from Eq. (25). In Fig. 1 we have provided a Kruskal diagram depicting the null rays in a (1+1) dimensional Schwarzschild black hole spacetime, and in this figure one also notices that d distinguishes different outgoing null paths. We mention that, utilizing quantum field theory one can perceive particle production in conformal Boulware vacuum with respect to observers, moving along these null paths [58, 59].

On the other hand, the outgoing and ingoing null coordinates in a general de Sitter background is given by $u = \eta - |\vec{x}|$ and $v = \eta + |\vec{x}|$. One can simply understand that these expressions in (1+1) dimensions become $u = \eta - x$ and $v = \eta + x$. With respect to the coordinate time t an observer along these null paths perceives the conformal vacuum particle generating. The scenarios of particle creation in curved spacetimes also influences the entanglement related observations. Therefore, we are going to consider these null trajectories in the Schwarzschild and FLRW spacetimes to understand the entanglement harvesting conditions from the relevant conformal vacuums.

V. GREEN'S FUNCTION CORRESPONDING TO OUTGOING NULL DETECTORS

From Eq. (7) and (4) of Sec. II we have seen that it is imperative to construct the Green's functions for a considered trajectory in a background spacetime to understand the entanglement harvesting conditions in this scenario. In this section, we will construct these necessary Green's functions along the null paths in the previously considered Schwarzschild and FLRW spacetimes. In this regard, we mention that rather than considering these Green's functions in their position space representations, we will take them in their momentum space representations. This consideration allows one to evaluate detector transition probabilities corresponding to a specific field mode frequency even with linear field-detector interaction in (1 + 1) dimensions. With this particular consideration, we also observed that one could circumvent the issues related to the infrared cutoff inherent to the (1 + 1) dimensional massless scalar field theory.

A. Schwarzschild background

1. Boulware vacuum

The positive frequency Boulware modes in terms of the null coordinates u and v are given by $e^{-i\omega u}$ and $e^{-i\omega v}$. One can then decompose a massless minimally coupled scalar field Φ in terms of these Boulware modes and suitably choosing the sets of creation and annihilation operators $\{\hat{a}_k^{B\dagger}, \hat{a}_k^B\}$ and $\{\hat{b}_k^{B\dagger}, \hat{b}_k^B\}$ as [74]

$$\Phi = \int_0^\infty \frac{d\omega_k}{\sqrt{4\pi\omega_k}} \left[\hat{a}_k^B e^{-i\omega_k u} + \hat{a}_k^{B\dagger} e^{i\omega_k u} + \hat{b}_k^B e^{-i\omega_k v} + \hat{b}_k^{B\dagger} e^{i\omega_k v} \right]. \quad (27)$$

The ladder operators satisfy the commutation relation $[\hat{a}_k^B, \hat{a}_{k'}^{B\dagger}] = \delta_{k,k'}$ and $[\hat{b}_k^B, \hat{b}_{k'}^{B\dagger}] = \delta_{k,k'}$, where all other choices in the commutator vanishes. Also the Boulware vacuum $|0\rangle_B$ is now defined by the one annihilated by these annihilation operators $\hat{a}_k^B |0\rangle_B = 0 = \hat{b}_k^B |0\rangle_B$. Then using the above field decomposition one can get the positive frequency Wightman function with respect to the Boulware vacuum to be given by

$$\begin{aligned} G_B^+(X_j, X_l) &= {}_B\langle 0 | \Phi(X_j) \Phi(X_l) | 0 \rangle_B \\ &= \int_0^\infty \frac{d\omega_k}{4\pi\omega_k} [e^{-i\omega_k(u_j - u_l)} + e^{-i\omega_k(v_j - v_l)}], \end{aligned} \quad (28)$$

where the subscript j and l correspond to the events X_j and X_l respectively.

Now we shall be considering one detector, say detector A with a non zero d , and detector B with $d = 0$. Then we shall be using $t_A = r_A + 2r_H \ln[r_A/r_H - 1] + d$ and $t_B = r_B + 2r_H \ln[r_B/r_H - 1]$. Using these EF coordinates, for

two detectors following outgoing null trajectories (26), one has the quantities

$$\begin{aligned} v'_j - v_l &= t'_{s_j} + r'_{*j} - (t_{s_l} + r_{*l}) \\ &= 2(r'_j - r_l) + 2r_H \ln \left[\frac{r'_j - r_H}{r_l - r_H} \right] \\ &\quad + d(\delta_{jA} \delta_{lB} - \delta_{jB} \delta_{lA}), \end{aligned} \quad (29)$$

and

$$\begin{aligned} u'_j - u_l &= t'_{s_j} - r'_{*j} - (t_{s_l} - r_{*l}) \\ &= d(\delta_{jA} \delta_{lB} - \delta_{jB} \delta_{lA}), \end{aligned} \quad (30)$$

where j and l can represent either detector A or B , with δ_{jl} denoting the *Kronecker delta* defined as

$$\begin{aligned} \delta_{jl} &= 0, \quad \text{if } j \neq l \\ &= 1, \quad \text{if } j = l. \end{aligned} \quad (31)$$

Substitution of (29) and (30) in (28) provides us the required Green's function G_B^+ corresponding to the Boulware vacuum with respect to our observers.

2. Unruh vacuum

To discuss about the Unruh modes and the corresponding Unruh vacuum one needs an understanding of the Kruskal coordinates $V = 2r_H e^{v/2r_H}$, and $U = -2r_H e^{-u/2r_H}$. Then the positive frequency Unruh modes in terms of the null coordinates v and U are given by $e^{-i\omega U}$ and $e^{-i\omega v}$. In terms of these Unruh modes a massless minimally coupled scalar field Φ is decomposed, choosing the sets of creation and annihilation operators $\{\hat{a}_k^{U\dagger}, \hat{a}_k^U\}$ and $\{\hat{b}_k^{U\dagger}, \hat{b}_k^U\}$, as

$$\Phi = \int_0^\infty \frac{d\omega_k}{\sqrt{4\pi\omega_k}} \left[\hat{a}_k^U e^{-i\omega_k v} + \hat{a}_k^{U\dagger} e^{i\omega_k v} + \hat{b}_k^U e^{-i\omega_k U} + \hat{b}_k^{U\dagger} e^{i\omega_k U} \right]. \quad (32)$$

The ladder operators satisfy the commutation relation $[\hat{a}_k^U, \hat{a}_{k'}^{U\dagger}] = \delta_{k,k'}$ and $[\hat{b}_k^U, \hat{b}_{k'}^{U\dagger}] = \delta_{k,k'}$, where all other choices in the commutator vanishes. Also the Unruh vacuum $|0\rangle_U$ is now defined by the one annihilated by these annihilation operators $\hat{a}_k^U |0\rangle_U = 0 = \hat{b}_k^U |0\rangle_U$. Then using the above field decomposition one can get the positive frequency Wightman function with respect to the Unruh vacuum to be given by

$$\begin{aligned} G_U^+(X_j, X_l) &= {}_U\langle 0 | \Phi(X_j) \Phi(X_l) | 0 \rangle_U \\ &= \int_0^\infty \frac{d\omega_k}{4\pi\omega_k} [e^{-i\omega_k(v_j - v_l)} + e^{-i\omega_k(U_j - U_l)}], \end{aligned} \quad (33)$$

where the subscript j and l correspond to the events X_j and X_l respectively. To write this in terms of our chosen trajectories we need to use the following transformation

relations. Using the EF coordinates, for two detectors in outgoing null trajectories (26), one has these relations

$$\begin{aligned} v'_j - v_l &= t'_{s_j} + r'_{*j} - (t_{s_l} + r_{*l}) \\ &= 2(r'_j - r_l) + 2r_H \ln \left[\frac{r'_j - r_H}{r_l - r_H} \right] \\ &\quad + d(\delta_{jA} \delta_{lB} - \delta_{jB} \delta_{lA}), \end{aligned} \quad (34)$$

and

$$\begin{aligned} U'_j - U_l &= -2r_H e^{-\frac{u'_j}{2r_H}} - (-2r_H e^{-\frac{u_l}{2r_H}}) \\ &= 2r_H \left(1 - e^{-\frac{d}{2r_H}} \right) (\delta_{jA} \delta_{lB} - \delta_{jB} \delta_{lA}). \end{aligned} \quad (35)$$

B. de Sitter spacetime

1. (1+1)-dimensions

Let us consider a massless minimally coupled scalar field Φ in the (1 + 1) dimensional de Sitter background denoted by (22). In particular, the equation of motion for the field Φ suggests field mode solutions of the form $u_\nu = e^{\mp i\omega_k(\eta \mp x)}$. Let us construct like the Schwarzschild case the outgoing and ingoing null coordinates $u = \eta - x$ and $v = \eta + x$. Then with a suitable set of creation and annihilation operators and with these mode functions one can decompose the scalar field as

$$\begin{aligned} \Phi &= \int_0^\infty \frac{d\omega_k}{\sqrt{4\pi\omega_k}} \left[\hat{a}_k^D e^{-i\omega_k u} + \hat{a}_k^{D\dagger} e^{i\omega_k u} \right. \\ &\quad \left. + \hat{b}_k^D e^{-i\omega_k v} + \hat{b}_k^{D\dagger} e^{i\omega_k v} \right], \end{aligned} \quad (36)$$

where the annihilation operators \hat{a}_k^D and \hat{b}_k^D annihilate the de Sitter vacuum $|0\rangle_D$. Then with the help of this field decomposition one can express the Green's function as

$$\begin{aligned} G_D^+(X_j, X_l) &= {}_D\langle 0 | \Phi(X_j) \Phi(X_l) | 0 \rangle_D \\ &= \int_0^\infty \frac{d\omega_k}{4\pi\omega_k} \left[e^{-i\omega_k(u_j - u_l)} + e^{-i\omega_k(v_j - v_l)} \right]. \end{aligned} \quad (37)$$

We also mention that along outgoing null trajectory $u = \eta - x$ is constant and along an ingoing null trajectory $v = \eta + x$ is constant. We consider our two observers Alice and Bob moving in outgoing null trajectories, and for Alice $\eta = x + d$ while for Bob $\eta = x$. With the help of Kronecker delta δ_{jl} one can collectively express these differences as

$$\begin{aligned} u_j - u_l &= d(\delta_{jA} \delta_{lB} - \delta_{jB} \delta_{lA}) \\ v_j - v_l &= 2\alpha_d (e^{-t_l/\alpha_d} - e^{-t_j/\alpha_d}) \\ &\quad - d(\delta_{jA} \delta_{lB} - \delta_{jB} \delta_{lA}), \end{aligned} \quad (38)$$

where, j and l can take values of either A or B . Substituting (38) in (37) we will find our required G_D^+ with respect to the outgoing trajectory.

2. (1+3)-dimensions

In (1 + 3) dimensional de Sitter spacetime also the conformal factor is $\Omega = a(\eta)$ like (1 + 1) dimensions. However, the difference in the spacetime dimensionality results in a factor of $a(\eta)^{(2-4)/2}$ in the scalar field decomposition of (16). In particular, in a (1 + 3)-dimensional FLRW universe a conformally coupled scalar field Φ can be decomposed into modes and ladder operators as,

$$\begin{aligned} \Phi &= \int \frac{d^3k}{\sqrt{(2\pi)^3 2\omega_k}} \frac{1}{a(\eta)} \left(e^{-i\omega_k \eta + i\vec{k} \cdot \vec{x}} \hat{b}_{\vec{k}, \omega_k}^- \right. \\ &\quad \left. + e^{i\omega_k \eta - i\vec{k} \cdot \vec{x}} \hat{b}_{\vec{k}, \omega_k}^+ \right). \end{aligned} \quad (39)$$

For simplicity, we choose the detectors to be outgoing along the x axis. Then along this path $\Delta y = 0 = \Delta z$, and only the k_x component from the factor $\vec{k} \cdot \vec{x}$ will survive in the Green's function evaluated with respect to the conformal vacuum. The Wightman functions for these outgoing null paths are given by

$$G_W(X_j, X_l) = \int \frac{d^3k}{(2\pi)^3 2\omega_k} \frac{e^{ik_x \Delta x_{jl} - i\omega_k \Delta \eta_{jl}}}{a(\eta_j) a(\eta_l)}. \quad (40)$$

For the case when the detectors are moving along the x axis, i.e., the motion of the detectors are actually confined to a one dimensional line, the outgoing null paths corresponding to Alice and Bob are again $\eta = x + d$ and $\eta = x$. One can use the information of these paths to obtain the appropriate Δx_{jl} and $\Delta \eta_{jl}$ in a straightforward manner. Then one can substitute these expressions in (40) to obtain the necessary Green's functions in the null trajectories.

VI. ENTANGLEMENT HARVESTING

A. Schwarzschild background

1. Boulware vacuum

As we have already discussed we are considering one detector, say detector A with a non zero d , and detector B with $d = 0$. First we shall use the expression of the Wightman function estimated in the Boulware vacuum from Eq. (28). With the coordinate transformations of Eq. (29) and (30) suitable to an observer in an outgoing null path in a Schwarzschild black hole spacetime, one can compute the necessary integrals of (7) to investigate the entanglement harvesting condition. In particular, one can find out the individual detector transition probabilities \mathcal{I}_j as

$$\begin{aligned} \mathcal{I}_j &= \int_{-\infty}^\infty dt'_j \int_{-\infty}^\infty dt_j e^{-i\Delta E^j(t'_j - t_j)} G_B^+(X'_j, X_j) \\ &= \int_0^\infty \frac{d\omega_k}{4\pi\omega_k} \mathcal{I}_{j\omega_k}. \end{aligned} \quad (41)$$

Here the integrals $\mathcal{I}_{j\omega_k}$ are represented as

$$\begin{aligned}\mathcal{I}_{j\omega_k} &= \int_{-\infty}^{\infty} dt'_j \int_{-\infty}^{\infty} dt_j e^{-i\Delta E^j(t'_j-t_j)} \\ &\quad \times [e^{-i\omega_k(u_{j'}-u_j)} + e^{-i\omega_k(v_{j'}-v_j)}] \\ &= \int_{-\infty}^{\infty} dt'_j \int_{-\infty}^{\infty} dt_j e^{-i\Delta E^j(t'_j-t_j)} \\ &\quad \times \left[1 + e^{-2i\omega_k(r_{j'}-r_j)} \left(\frac{r_{j'}-r_H}{r_j-r_H} \right)^{-2ir_H\omega_k} \right],\end{aligned}\quad (42)$$

where we have used the relations from Eq. (29) and (30). Here we mention that the integrations over the first additive unity provides multiplicative factors of the Dirac delta distributions $\delta(\Delta E^j)$, which makes the contribution of that part of the integration to vanish as the detector transition energy $\Delta E^j > 0$. Then we consider the expression of (25) for the realization of outgoing null paths in this calculation and the expression (42) transforms into

$$\begin{aligned}\mathcal{I}_{j\omega_k} &= \int_{r_H}^{\infty} dr_{j'} \frac{r_{j'}+r_H}{r_{j'}-r_H} \int_{r_H}^{\infty} dr_j \frac{r_j+r_H}{r_j-r_H} \\ &\quad \times e^{-i(\Delta E^j+2\omega_k)(r_{j'}-r_j)} \left(\frac{r_{j'}-r_H}{r_j-r_H} \right)^{-2ir_H(\Delta E^j+\omega_k)}\end{aligned}\quad (43)$$

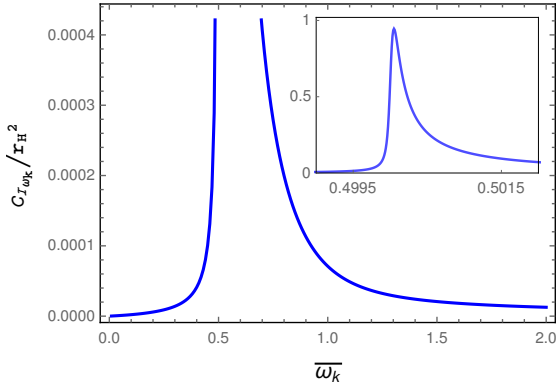


FIG. 2: The quantity $\mathcal{C}_{\mathcal{I}_{\omega_k}}/r_H^2 = (|\mathcal{I}_{\varepsilon\omega_k}| - \mathcal{I}_{j\omega_k})/r_H^2$, signifying the concurrence, is plotted for two outgoing null detectors in a (1 + 1) dimensional Schwarzschild black hole spacetime with respect to the dimensionless frequency of the field $\bar{\omega}_k = r_H\omega_k$ for fixed detector transition energies $\Delta E^A = r_H\Delta E^A = 1$, $\Delta E^B = r_H\Delta E^B = 1$, and $d = 0$.

Now one may consider a change of variables $y'_j = r_{j'}/r_H - 1$ and $y_j = r_j/r_H - 1$. Then this integral simplifies to

$$\mathcal{I}_{j\omega_k} = r_H^2 \left| \int_0^{\infty} dy_j \frac{y_j + 2}{y_j} \frac{e^{ir_H(\Delta E^j+2\omega_k)y_j}}{y_j^{-2ir_H(\Delta E^j+\omega_k)}} \right|^2.\quad (44)$$

To evaluate this integral we introduce regulator of the form $y_j^\epsilon e^{-\epsilon y_j}$, where ϵ is a real positive parameter. Then

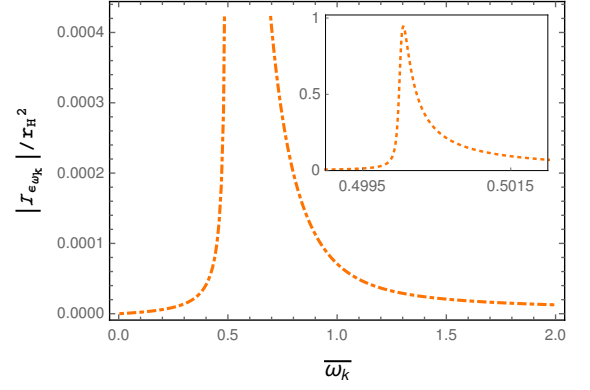


FIG. 3: The quantity $|\mathcal{I}_{\varepsilon\omega_k}|/r_H^2$ is plotted for two outgoing null detectors in a (1 + 1) dimensional Schwarzschild black hole spacetime with respect to the frequency of the field $\bar{\omega}_k = r_H\omega_k$ for fixed detector transition energies $\Delta E^A = r_H\Delta E^A = 1$, $\Delta E^B = r_H\Delta E^B = 1$, and $d = 0$.

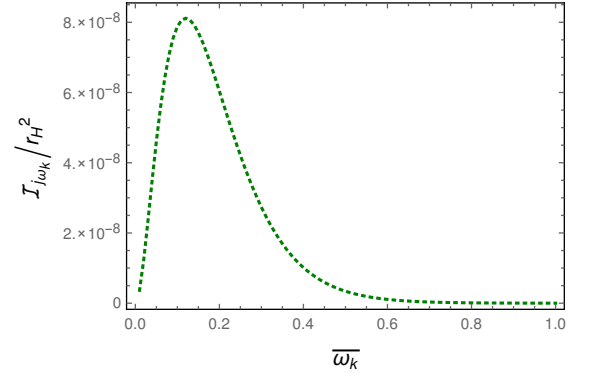


FIG. 4: The quantity $\mathcal{I}_{j\omega_k}/r_H^2$ is plotted for two outgoing null detectors in a (1 + 1) dimensional Schwarzschild black hole spacetime with respect to the frequency of the field $\bar{\omega}_k = r_H\omega_k$ for fixed detector transition energies $\Delta E^A = r_H\Delta E^A = 1$, $\Delta E^B = r_H\Delta E^B = 1$, and $d = 0$.

the actual value of the integral is obtained by taking the limit $\epsilon \rightarrow 0$ after evaluating the regulated integral as

$$\begin{aligned}\lim_{\epsilon \rightarrow 0} &\left[\int_0^{\infty} dy_j \frac{y_j + 2}{y_j} \frac{e^{ir_H(\Delta E^j+2\omega_k)y_j - \epsilon y_j}}{y_j^{-2ir_H(\Delta E^j+\omega_k) - \epsilon}} \right] \\ &= e^{-\pi r_H(\Delta E^j+\omega_k)} \Gamma(2ir_H(\Delta E^j+\omega_k)) \\ &\quad \times \frac{2\omega_k (r_H(\Delta E^j+2\omega_k))^{-2ir_H(\Delta E^j+\omega_k)}}{\Delta E^j+2\omega_k}.\end{aligned}\quad (45)$$

The entire integral $\mathcal{I}_{j\omega_k}$ from (45) becomes

$$\begin{aligned}\mathcal{I}_{j\omega_k} &= \frac{4\pi r_H\omega_k^2}{(\Delta E^j+\omega_k)(\Delta E^j+2\omega_k)^2} \\ &\quad \times \frac{1}{e^{4\pi r_H(\Delta E^j+\omega_k)} - 1},\end{aligned}\quad (46)$$

where we have used the *Gamma function* identity $\Gamma(iz)\Gamma(-iz) = \pi/(z \sinh \pi z)$. This signifies a somewhat

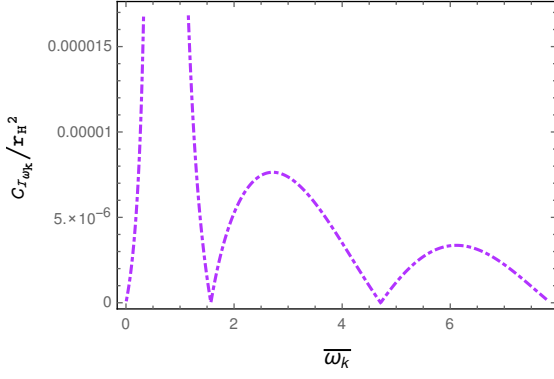


FIG. 5: The quantity $C_{\mathcal{I}_{\omega_k}}/r_H^2$ is plotted for two outgoing null detectors in different parallel paths in a (1 + 1) dimensional Schwarzschild black hole spacetime with respect to the frequency of the field $\bar{\omega}_k$ for fixed detector transition energy $\overline{\Delta E} = 1$, and $d/r_H = 1$.

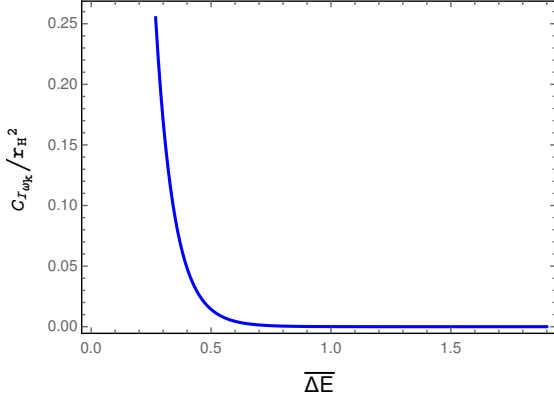


FIG. 6: The quantity $C_{\mathcal{I}_{\omega_k}}/r_H^2$ is plotted for two outgoing null detectors in a (1 + 1) dimensional Schwarzschild black hole spacetime with respect to the dimensionless transition energy $\overline{\Delta E} = r_H \Delta E$ of the detectors, where $\Delta E = \Delta E^A = \Delta E^B$. The dimensionless field mode frequency is fixed at $\bar{\omega}_k = 1$ and $d = 0$.

Planckian distribution with respect to the detector transition energy ΔE^j plus energy of each Boulware mode ω_k . On the other hand, for the evaluation of the integral \mathcal{I}_ε we express it with the help of Eq. (8) as

$$\mathcal{I}_\varepsilon = -\mathcal{I}_\varepsilon^W - \mathcal{I}_\varepsilon^R, \quad (47)$$

where one has

$$\begin{aligned} \mathcal{I}_\varepsilon^W &= \int_{-\infty}^{\infty} d\tau_B \int_{-\infty}^{\infty} d\tau_A e^{i(\Delta E^B \tau_B + \Delta E^A \tau_A)} G_W(X_B, X_A) \\ &= \int_0^{\infty} \frac{d\omega_k}{4\pi\omega_k} \mathcal{I}_{\varepsilon\omega_k}^W, \end{aligned} \quad (48)$$

and

$$\begin{aligned} \mathcal{I}_\varepsilon^R &= \int_{-\infty}^{\infty} d\tau_B \int_{-\infty}^{\infty} d\tau_A e^{i(\Delta E^B \tau_B + \Delta E^A \tau_A)} \theta(T_A - T_B) \\ &\quad \times [G_W(X_A, X_B) - G_W(X_B, X_A)] \end{aligned}$$

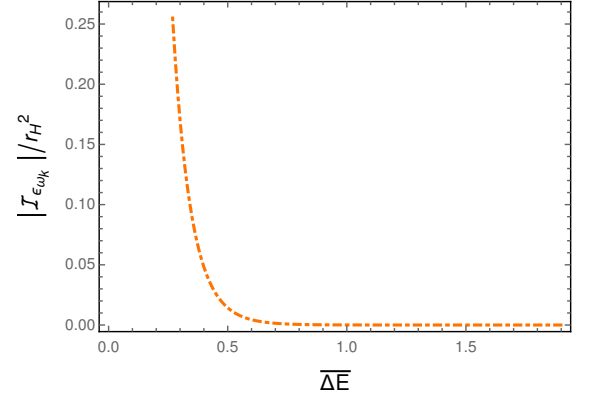


FIG. 7: The quantity $|\mathcal{I}_{\varepsilon\omega_k}|/r_H^2$ is plotted for two outgoing null detectors in a (1+1) dimensional Schwarzschild black hole spacetime with respect to the dimensionless transition energy $\overline{\Delta E} = r_H \Delta E$ of the detectors, where $\Delta E = \Delta E^A = \Delta E^B$. The dimensionless field mode frequency is fixed at $\bar{\omega}_k = 1$ and $d = 0$.

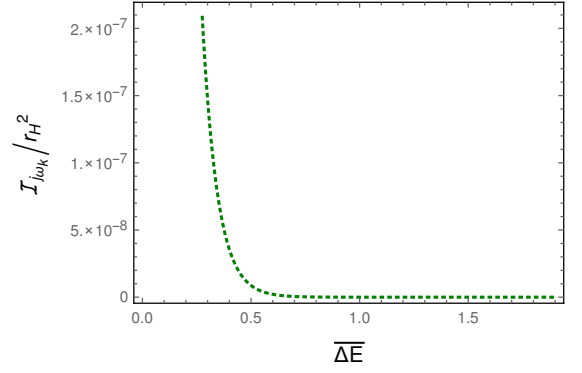


FIG. 8: The quantity $\mathcal{I}_{j\omega_k}/r_H^2$ is plotted for two outgoing null detectors in a (1 + 1) dimensional Schwarzschild black hole spacetime with respect to the dimensionless transition energy $\overline{\Delta E} = r_H \Delta E$ of the detectors, where $\Delta E = \Delta E^A = \Delta E^B$. The dimensionless field mode frequency is fixed at $\bar{\omega}_k = 1$ and $d = 0$.

$$= \int_0^{\infty} \frac{d\omega_k}{4\pi\omega_k} \mathcal{I}_{\varepsilon\omega_k}^R. \quad (49)$$

One should note here the detector times τ_j are denoted by the EF times, i.e., $\tau_j = t_j$. On the other hand, the times T_j appearing in the Heaviside step function due to field decomposition are the Schwarzschild times t_{s_j} as the field decomposition has been done with respect to the Boulware modes. With the help of Eq. (29) and (30) one can express the integral $\mathcal{I}_{\varepsilon\omega_k}^W$ as

$$\begin{aligned} \mathcal{I}_{\varepsilon\omega_k}^W &= \int_{-\infty}^{\infty} dt_B \int_{-\infty}^{\infty} dt_A e^{i(\Delta E^B t_B + \Delta E^A t_A)} \\ &\quad \times [e^{-i\omega_k(u_B - u_A)} + e^{-i\omega_k(v_B - v_A)}] \\ &= \int_{-\infty}^{\infty} dt_B \int_{-\infty}^{\infty} dt_A e^{i(\Delta E^B t_B + \Delta E^A t_A)} \left[e^{i\omega_k d} \right. \end{aligned}$$

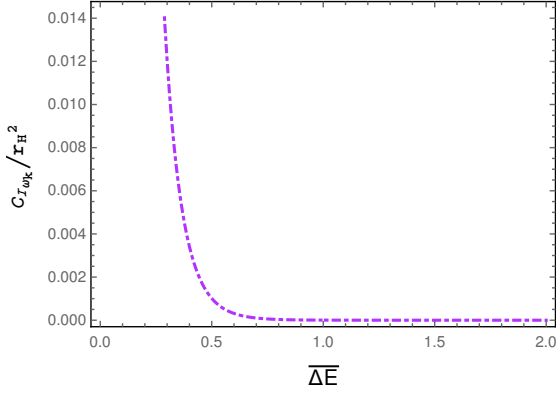


FIG. 9: The quantity $\mathcal{C}_{\mathcal{I}_{\omega_k}}/r_H^2$ is plotted for two outgoing null detectors in different parallel paths in a (1 + 1) dimensional Schwarzschild black hole spacetime with respect to the dimensionless detector transition energy $\overline{\Delta E}$ for fixed frequency of the field $\bar{\omega}_k = 1$ and $d/r_H = 1.5$.

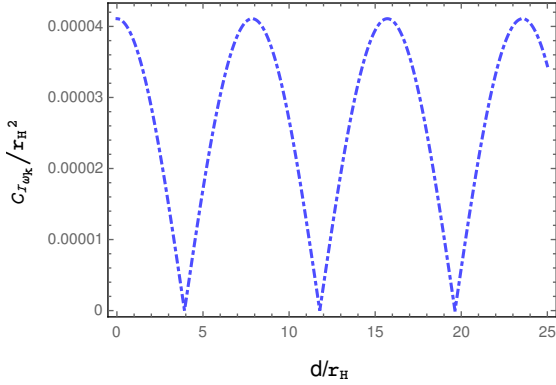


FIG. 10: The quantity $\mathcal{C}_{\mathcal{I}_{\omega_k}}/r_H^2$ is plotted for two outgoing null detectors in different parallel paths in a (1 + 1) dimensional Schwarzschild black hole spacetime with respect to the separation between the two paths d/r_H . The frequency of the field and the detector transition energies are fixed at $\bar{\omega}_k = 0.4$ and $\overline{\Delta E} = 1$.

$$+e^{-i\omega_k(2r_B-2r_A-d)} \left(\frac{r_B - r_H}{r_A - r_H} \right)^{-2ir_H\omega_k} \Big]. \quad (50)$$

Here also one can observe that the integration over the first quantity with $e^{i\omega_k d}$ as multiplicative factor will provide the multiplication of Dirac delta distributions $\delta(\Delta E^A)$ and $\delta(\Delta E^B)$. Therefore that part of the integral will vanish as the detector transition energy $\Delta E^j > 0$. Now like the evaluation of $\mathcal{I}_{j\omega_k}$ we utilize Eq. (26) and consider a change of variables $y_B = r_B/r_H - 1$ and $y_A = r_A/r_H - 1$, which will simplify the above integral to

$$\begin{aligned} \mathcal{I}_{\varepsilon\omega_k}^W &= r_H^2 e^{id(\Delta E^A + \omega_k)} \\ &\times \left[\int_0^\infty dy_B \frac{y_B + 2}{y_B} \frac{e^{ir_H(\Delta E^B - 2\omega_k)(y_B + 1)}}{y_B^{-2ir_H(\Delta E^B - \omega_k)}} \right. \end{aligned}$$

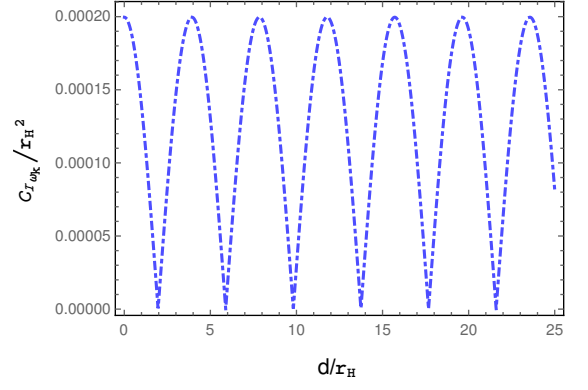


FIG. 11: The quantity $\mathcal{C}_{\mathcal{I}_{\omega_k}}/r_H^2$ is plotted for two outgoing null detectors in different parallel paths in a (1 + 1) dimensional Schwarzschild black hole spacetime with respect to the separation between the two paths d/r_H . The frequency of the field and the detector transition energies are fixed at $\bar{\omega}_k = 0.8$ and $\overline{\Delta E} = 1$.

$$\times \int_0^\infty dy_A \frac{y_A + 2}{y_A} \frac{e^{ir_H(\Delta E^A + 2\omega_k)(y_A + 1)}}{y_A^{-2ir_H(\Delta E^A + \omega_k)}} \Big]. \quad (51)$$

The analytic expression of this integral (51) is given in Eq. (A1) of Appendix A 1. On the other hand, one can also express $\mathcal{I}_{\varepsilon}^R$, which contains the contribution from a retarded Green's function, from Eq. (49) as

$$\begin{aligned} \mathcal{I}_{\varepsilon\omega_k}^R &= \int_{-\infty}^\infty dt_A \int_{-\infty}^\infty dt_B e^{i(\Delta E^B t_B + \Delta E^A t_A)} \theta(t_{s_A} - t_{s_B}) \\ &\times [e^{-i\omega_k(u_A - u_B)} + e^{-i\omega_k(v_A - v_B)} \\ &- e^{-i\omega_k(u_B - u_A)} - e^{-i\omega_k(v_B - v_A)}] . \quad (52) \end{aligned}$$

Here we mention that the Schwarzschild time t_s and the EF time t are related among themselves as $t + r = t_s + r_*$. Along an outgoing null trajectory (26) one readily gets $\theta(t_{s_A} - t_{s_B}) = \theta(r_{*A} + d - r_{*B})$. Then for any $d > 0$ as one takes $r_A > r_B$ the outcome $t_{s_A} > t_{s_B}$ is guaranteed, i.e., $\theta(r_A - r_B) \Rightarrow \theta(t_{s_A} - t_{s_B})$ for $d > 0$. In our analysis we have considered $d > 0$, transformed the coordinate t to r using relation (26), and utilized the $\theta(r_A - r_B)$ expression to change the limit of r_B to $[r_H, r_A]$ from $[r_H, \infty)$. Then one can proceed to evaluate the integral of (52) as

$$\begin{aligned} \mathcal{I}_{\varepsilon\omega_k}^R &= \int_{r_H}^\infty dr_A \frac{r_A + r_H}{r_A - r_H} \int_{r_H}^{r_A} dr_B \frac{r_B + r_H}{r_B - r_H} \\ &\times e^{i\{\Delta E^B r_B + \Delta E^A (r_A + d)\}} \left(\frac{r_B}{r_H} - 1 \right)^{2ir_H \Delta E^B} \\ &\times \left(\frac{r_A}{r_H} - 1 \right)^{2ir_H \Delta E^A} \left[e^{-i\omega_k(2r_A + d - 2r_B)} \right. \\ &\times \left(\frac{r_A - r_H}{r_B - r_H} \right)^{-2ir_H \omega_k} - e^{-i\omega_k(2r_B - 2r_A - d)} \\ &\times \left(\frac{r_B - r_H}{r_A - r_H} \right)^{-2ir_H \omega_k} - 2i \sin(\omega_k d) \Big]. \quad (53) \end{aligned}$$

Here we notice that the contribution from the quantity $e^{-i\omega_k(u_A - u_B)} - e^{-i\omega_k(u_B - u_A)} = -2i \sin(\omega_k d)$ is independent of t_j . With the change of variables $y_B = r_B/r_H - 1$ and $y_A = r_A/r_H - 1$, the above integral simplifies to

$$\begin{aligned} \mathcal{I}_{\varepsilon\omega_k}^R &= r_H^2 \left[e^{-i\omega_k d} \int_0^\infty dy_A \frac{y_A + 2}{y_A} \frac{e^{ir_H(\Delta E^A - 2\omega_k)(y_A + 1)}}{y_A^{-2ir_H(\Delta E^A - \omega_k)}} \right. \\ &\quad \int_0^{y_A} dy_B \frac{y_B + 2}{y_B} \frac{e^{ir_H(\Delta E^B + 2\omega_k)(y_B + 1)}}{y_B^{-2ir_H(\Delta E^B + \omega_k)}} \\ &\quad - e^{i\omega_k d} \int_0^\infty dy_A \frac{y_A + 2}{y_A} \frac{e^{ir_H(\Delta E^A + 2\omega_k)(y_A + 1)}}{y_A^{-2ir_H(\Delta E^A + \omega_k)}} \\ &\quad \int_0^{y_A} dy_B \frac{y_B + 2}{y_B} \frac{e^{ir_H(\Delta E^B - 2\omega_k)(y_B + 1)}}{y_B^{-2ir_H(\Delta E^B - \omega_k)}} \\ &\quad - 2i \sin(\omega_k d) \int_0^\infty dy_A \frac{y_A + 2}{y_A} \frac{e^{ir_H \Delta E^A (y_A + 1)}}{y_A^{-2ir_H \Delta E^A}} \\ &\quad \left. \int_0^{y_A} dy_B \frac{y_B + 2}{y_B} \frac{e^{ir_H \Delta E^B (y_B + 1)}}{y_B^{-2ir_H \Delta E^B}} \right]. \quad (54) \end{aligned}$$

One may go through Appendix A 1, Eq. (A2), for an analytical evaluation of this integral, which we have estimated introducing regulators. These regulators make the otherwise divergent integrals convergent. One gets the analytical expression of this integral in terms of the *Gamma functions* $\Gamma(x)$ and *Hypergeometric functions* ${}_2F_1(x)$. We also mention that the quantity with a multiplicative $2i \sin(\omega_k d)$ term here has negligible contribution compared to the other terms, see Appendix A 2.

Like the concurrence defined in Eq. (10) one perceives that in the symmetric case the quantity $\mathcal{C}_{\mathcal{I}_{\omega_k}} = (|\mathcal{I}_{\varepsilon\omega_k}| - \mathcal{I}_{j\omega_k})$ represents the concurrence corresponding to a specific field mode frequency ω_k , where $\mathcal{I}_{\varepsilon\omega_k} = \mathcal{I}_{\varepsilon\omega_k}^W + \mathcal{I}_{\varepsilon\omega_k}^R$. In Fig. 2 we have plotted the dimensionless quantity $\mathcal{C}_{\mathcal{I}_{\omega_k}}/r_H^2$, which represents the concurrence, with respect to the dimensionless parameter $\bar{\omega}_k = r_H \omega_k$ for fixed $\overline{\Delta E^A} = r_H \Delta E^A = 1$, $\overline{\Delta E^B} = r_H \Delta E^B = 1$, and $d = 0$. This plot clearly asserts that in this scenario entanglement harvesting is possible within a range of $\bar{\omega}_k$, and major contribution in concurrence comes from $|\mathcal{I}_{\varepsilon\omega_k}|$ rather than $\mathcal{I}_{j\omega_k}$, see Fig. 3 and 4. Furthermore, in Fig. 5 the dimensionless quantity $\mathcal{C}_{\mathcal{I}_{\omega_k}}/r_H^2$ is plotted with respect to the same parameter $\bar{\omega}_k$ for fixed $d/r_H = 1$, $\overline{\Delta E^A} = 1$, and $\overline{\Delta E^B} = 1$. From this plot also one can observe that entanglement harvesting is possible, but there is a notion of periodicity and the maximum amount of the harvested entanglement dampens as $\bar{\omega}_k$ increases in successive periods.

On the other hand, in Fig. 6 we have plotted $\mathcal{C}_{\mathcal{I}_{\omega_k}}/r_H^2$ with respect to the dimensionless transition energy $\overline{\Delta E} = r_H \Delta E$ of the detectors for fixed $\bar{\omega}_k = 1$ and $d = 0$, where $\Delta E = \Delta E^A = \Delta E^B$. This plot also proclaims the possibility of entanglement harvesting for small values of ΔE from the Boulware vacuum with two detectors moving along outgoing null trajectories in a Schwarzschild

black hole spacetime. Fig. 7 and Fig. 8 confirm that major contribution in concurrence comes from $|\mathcal{I}_{\varepsilon\omega_k}|$ rather than $\mathcal{I}_{j\omega_k}$. Moreover, in Fig. 9 the quantity $\mathcal{C}_{\mathcal{I}_{\omega_k}}/r_H^2$ is plotted with respect to the same parameter $\overline{\Delta E}$ for fixed $\bar{\omega}_k = 1$ and $d/r_H = 1.5$, which does not provide any new feature compared to the $d/r_H = 0$ case. Both $d/r_H = 1.5$ and $d/r_H = 0$ cases show that the amount of harvested entanglement decreases with increasing detector transition energy and the radius of the event horizon of the black hole.

In Fig. 10 and 11 we have plotted $\mathcal{C}_{\mathcal{I}_{\omega_k}}/r_H^2$ with respect to the dimensionless distance d/r_H between the two detectors' null trajectories for fixed $\overline{\Delta E} = 1$ and different $\bar{\omega}_k = 0.4$ and $\bar{\omega}_k = 0.8$ respectively. These plots and corresponding numerical values confirm that entanglement harvesting is happening in a periodic manner with respect to d/r_H , with period depending on $\bar{\omega}_k$. We observe that the period decreases while the amplitude increases with increasing values of the field mode frequency $\bar{\omega}_k$. They also confirm that there are periodic d/r_H values where harvesting stops, i.e., $\mathcal{C}_{\mathcal{I}_{\omega_k}}/r_H^2$ becomes zero. These specific d/r_H points are like entanglement harvesting shadow regions perceived in [54]. However, in [54] the entanglement harvesting shadow regions are observed in a different context near the event horizon of a rotating BTZ black hole.

2. Unruh vacuum

Here we consider the Wightman function estimated with the Unruh vacuum from Eq. (33) to estimate integrals of (7) to investigate the entanglement harvesting condition. In particular, one can find out the individual detector transition probabilities \mathcal{I}_j as

$$\begin{aligned} \mathcal{I}_j &= \int_{-\infty}^\infty dt'_j \int_{-\infty}^\infty dt_j e^{-i\Delta E^j(t'_j - t_j)} G_B^+(X'_j, X_j) \\ &= \int_0^\infty \frac{d\omega_k}{4\pi\omega_k} \mathcal{I}_{j\omega_k}, \quad (55) \end{aligned}$$

where $\mathcal{I}_{j\omega_k}$ are now given by

$$\begin{aligned} \mathcal{I}_{j\omega_k} &= \int_{-\infty}^\infty dt'_j \int_{-\infty}^\infty dt_j e^{-i\Delta E^j(t'_j - t_j)} \\ &\quad \times [e^{-i\omega_k(U_{j'} - U_j)} + e^{-i\omega_k(v_{j'} - v_j)}]. \quad (56) \end{aligned}$$

With the help of Eq. (34) and (35) one can observe that this integral is same as the one from Eq. (43) of the Boulware vacuum case. Then this should also provide the same result of Eq. (46). Let us now evaluate the integrals $\mathcal{I}_{\varepsilon\omega_k}^W$ and $\mathcal{I}_{\varepsilon\omega_k}^R$ from (48) and (49) with the Green's functions (33) evaluated from the Unruh vacuum. First let us proceed to calculate $\mathcal{I}_{\varepsilon\omega_k}^W$, which in this case turns out to be

$$\begin{aligned}
\mathcal{I}_{\varepsilon\omega_k}^W &= \int_{-\infty}^{\infty} dt_B \int_{-\infty}^{\infty} dt_A e^{i(\Delta E^B t_B + \Delta E^A t_A)} [e^{-i\omega_k(U_B - U_A)} + e^{-i\omega_k(v_B - v_A)}] \\
&= \int_{-\infty}^{\infty} dt_B \int_{-\infty}^{\infty} dt_A e^{i(\Delta E^B t_B + \Delta E^A t_A)} \left[\exp \left\{ i\omega_k 2r_H \left(1 - e^{-\frac{d}{2r_H}} \right) \right\} + e^{-i\omega_k(2r_B - 2r_A - d)} \left(\frac{r_B - r_H}{r_A - r_H} \right)^{-2ir_H\omega_k} \right] \quad (57)
\end{aligned}$$

The integration with the first term inside the square bracket will vanish due to the Dirac delta distributions $\delta(\Delta E^j)$, with $\Delta E^j > 0$. Then this integral becomes ex-

actly same with the one for the Boulware vacuum from Eq. (51). On the other hand, in a similar manner one can evaluate the quantity $\mathcal{I}_{\varepsilon\omega_k}^R$ as

$$\begin{aligned}
\mathcal{I}_{\varepsilon\omega_k}^R &= \int_{-\infty}^{\infty} dt_A \int_{-\infty}^{\infty} dt_B e^{i(\Delta E^B t_B + \Delta E^A t_A)} \left[\theta(t_{s_A} - t_{s_B}) \{ e^{-i\omega_k(v_A - v_B)} - e^{-i\omega_k(v_B - v_A)} \} \right. \\
&\quad \left. + \theta(T_{K_A} - T_{K_B}) \{ e^{-i\omega_k(U_A - U_B)} - e^{-i\omega_k(U_B - U_A)} \} \right] \\
&= \int_{r_H}^{\infty} dr_A \frac{r_A + r_H}{r_A - r_H} \int_{r_H}^{r_A} dr_B \frac{r_B + r_H}{r_B - r_H} e^{i\{\Delta E^B r_B + \Delta E^A(r_A + d)\}} \left(\frac{r_B}{r_H} - 1 \right)^{2ir_H\Delta E^B} \left(\frac{r_A}{r_H} - 1 \right)^{2ir_H\Delta E^A} \\
&\quad \times \left[e^{-i\omega_k(2r_A + d - 2r_B)} \left(\frac{r_A - r_H}{r_B - r_H} \right)^{-2ir_H\omega_k} - e^{-i\omega_k(2r_B - 2r_A - d)} \left(\frac{r_B - r_H}{r_A - r_H} \right)^{-2ir_H\omega_k} - 2i \sin \left\{ \omega_k 2r_H \left(1 - e^{-\frac{d}{2r_H}} \right) \right\} \right]. \quad (58)
\end{aligned}$$

Here we note that while dealing with modes which are represented in terms of the EF null coordinates the Heaviside step function arising from the Feynman propagator should take the time to be the Schwarzschild time t_s . While for modes which are represented in terms of the Kruskal null coordinates (U, V) , one should take the relevant time to be the Kruskal time $T_K = (U + V)/2$. This Kruskal time is expressed in terms of the Schwarzschild time and the tortoise coordinate as $T_K = 2r_H e^{r_*/2r_H} \sinh(t_s/2r_H)$. Using this expression and the null paths followed by Alice and Bob as $t_{s_A} - r_{\star A} = d > 0$ and $t_{s_B} - r_{\star B} = 0$, respectively one finds that $T_{K_A} > T_{K_B}$ implies $r_A > r_B$ (see Appendix B). Therefore the Heaviside function $\theta(T_{K_A} - T_{K_B})$ can be replaced by $\theta(r_A - r_B)$. Similarly, as explained earlier, $t_{s_A} > t_{s_B}$ implies $r_A > r_B$ and hence we replace $\theta(t_{s_A} - t_{s_B})$ by $\theta(r_A - r_B)$. Using these the last result of (58) has been obtained. We observe that the expression of $\mathcal{I}_{\varepsilon\omega_k}^R$ from Eq. (58) and (54) are mathematically same except for the last term. In Appendix A 2 we have shown that this last term $2i \sin \left\{ \omega_k 2r_H \left(1 - e^{-d/2r_H} \right) \right\}$ is many order smaller than the rest of the expressions for the same set of parameter values. Therefore, the nature of entanglement harvesting with respect to the Unruh vacuum is similar to that in the Boulware vacuum.

B. de Sitter universe

1. (1 + 1)-dimensions

Let us now evaluate the integrals of Eq. (4) for detectors in null trajectories in a de Sitter spacetime, so that one can check the entanglement condition (7) and also quantify the harvested entanglement using (10). In this regard, we first consider the integral \mathcal{I}_j , which using the Green's function of Eq. (37) is represented as

$$\begin{aligned}
\mathcal{I}_j &= \int_{-\infty}^{\infty} dt'_j \int_{-\infty}^{\infty} dt_j e^{-i\Delta E^j(t'_j - t_j)} G_D^+(X_j, X_l) \\
&= \int_0^{\infty} \frac{d\omega_k}{4\pi\omega_k} \mathcal{I}_{j\omega_k}. \quad (59)
\end{aligned}$$

Here the detector times τ_j are represented by the de Sitter coordinate times t_j . Like the previous Schwarzschild case here also we shall be evaluating $\mathcal{I}_{j\omega_k}$, which correspond to a certain frequency of the field mode, to arrive at the entanglement harvesting condition. With the consideration of outgoing null paths for both Alice and Bob one can express the integrals $\mathcal{I}_{j\omega_k}$ as

$$\begin{aligned}
\mathcal{I}_{j\omega_k} &= \int_{-\infty}^{\infty} dt'_j \int_{-\infty}^{\infty} dt_j e^{-i\Delta E^j(t'_j - t_j)} \\
&\quad \times [e^{-2i\omega_k\alpha_d(e^{-t'_j/\alpha_d} - e^{-t_j/\alpha_d})} + 1]. \quad (60)
\end{aligned}$$

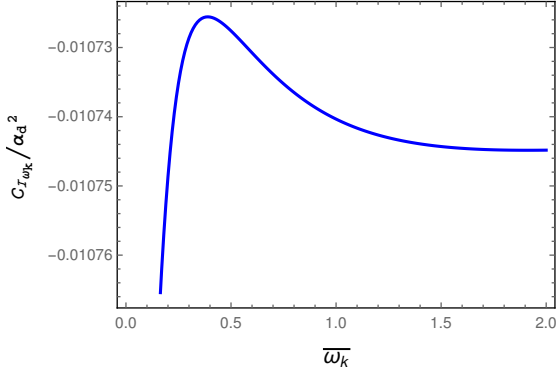


FIG. 12: The quantity $C_{I_{\omega_k}}/\alpha_d^2$, signifying the concurrence, is plotted for two outgoing null detectors in a (1 + 1) dimensional DeSitter spacetime with respect to the dimensionless frequency of the field $\bar{\omega}_k = \omega_k \alpha_d$ for fixed dimensionless detector transition energy $\Delta\bar{E} = \Delta E \alpha_d = 1$.

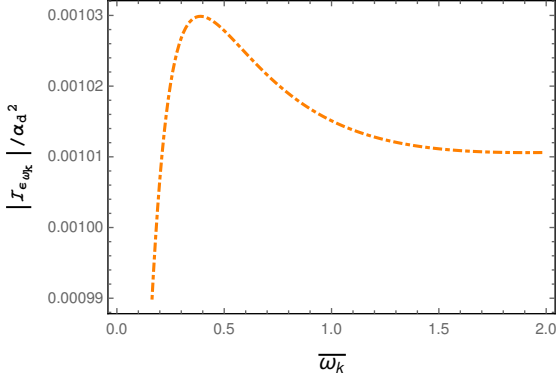


FIG. 13: The quantity $|I_{\epsilon_{\omega_k}}|/\alpha_d^2$ is plotted for two outgoing null detectors in a (1+1) dimensional DeSitter spacetime with respect to the dimensionless frequency of the field $\bar{\omega}_k$ for fixed $\Delta\bar{E} = 1$.

Here one can observe that the integration over the second additive unity is simple and provides multiplicative factors of the Dirac delta distribution $\delta(\Delta E^j)$. For non zero detector transition energy $\Delta E^j > 0$ these quantities are bound to make the concerned part of the integral vanish. Then the previous integral with the change of variables $e^{-t/\alpha_d} = z$ can be evaluated as

$$I_{j_{\omega_k}} = \alpha_d^2 \left| \int_0^\infty dz z^{i\Delta E^j \alpha_d - 1} e^{2i\omega_k \alpha_d z} \right|^2. \quad (61)$$

To evaluate this integral we introduce regulators of the form $(z^\epsilon e^{-\epsilon z})$, where ϵ is a positive real parameter with $\epsilon \ll 1$. One can get the actual value of the integral by taking the limit $\epsilon \rightarrow 0$ after evaluating the regulated integral as

$$\begin{aligned} & \lim_{\epsilon \rightarrow 0} \left[\int_0^\infty dz z^{i\Delta E^j \alpha_d - 1 + \epsilon} e^{(2i\omega_k \alpha_d - \epsilon)z} \right] \\ &= e^{-\pi \alpha_d \Delta E^j / 2} (2\omega_k \alpha_d)^{-i\alpha_d \Delta E^j} \Gamma(i\alpha_d \Delta E^j). \end{aligned} \quad (62)$$

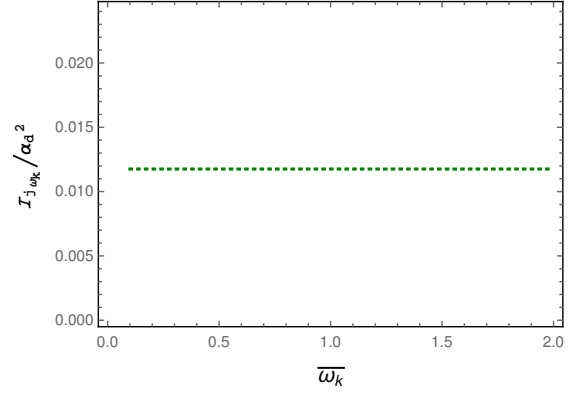


FIG. 14: The quantity $I_{j_{\omega_k}}/\alpha_d^2$, signifying the concurrence, is plotted for two outgoing null detectors in a (1 + 1) dimensional DeSitter spacetime with respect to the dimensionless frequency of the field $\bar{\omega}_k$ for fixed $\Delta\bar{E} = 1$.

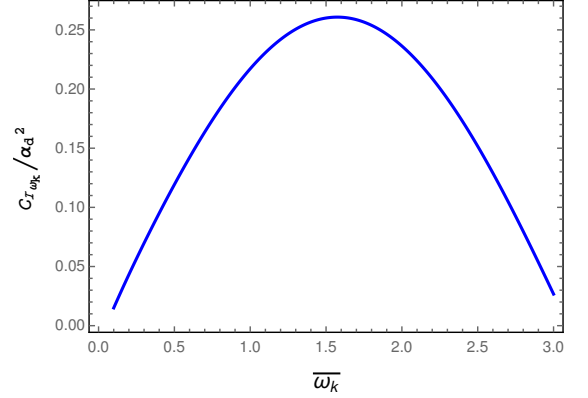


FIG. 15: The quantity $C_{I_{\omega_k}}/\alpha_d^2$, signifying the concurrence, is plotted for two outgoing null detectors in a (1 + 1) dimensional DeSitter spacetime with respect to the dimensionless frequency of the field $\bar{\omega}_k$ for fixed dimensionless detector transition energy $\Delta\bar{E} = 1$, and $d/\alpha_d = 1$.

Then one can promptly express $I_{j_{\omega_k}}$ as

$$I_{j_{\omega_k}} = \frac{2\pi\alpha_d}{\Delta E^j} \frac{1}{e^{2\pi\alpha_d \Delta E^j} - 1}, \quad (63)$$

where we have used the *Gamma function* identity $\Gamma(iz)\Gamma(-iz) = \pi/(z \sinh \pi z)$. Let us now evaluate the integral I_ϵ , which can again be expressed as

$$I_\epsilon = - \int_0^\infty \frac{d\omega_k}{4\pi\omega_k} \left[I_{\epsilon_{\omega_k}}^W + I_{\epsilon_{\omega_k}}^R \right], \quad (64)$$

which is in same way that we have considered in the Schwarzschild case. Here, one can evaluate the quantity $I_{\epsilon_{\omega_k}}^W$ as

$$\begin{aligned} I_{\epsilon_{\omega_k}}^W &= \int_{-\infty}^\infty dt_B \int_{-\infty}^\infty dt_A e^{i(\Delta E^A t_A + \Delta E^B t_B)} \\ &\times \left\{ e^{-i\omega_k(u_B - u_A)} + e^{-i\omega_k(v_B - v_A)} \right\} \end{aligned}$$

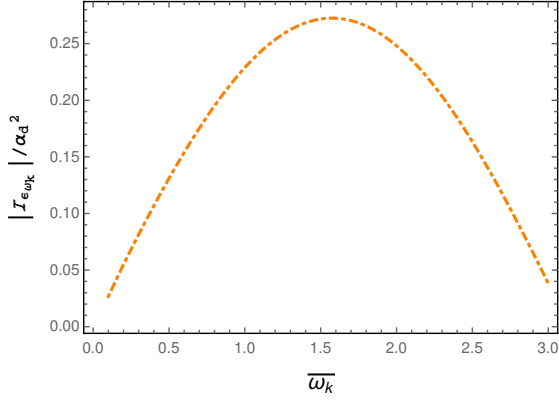


FIG. 16: The quantity $|\mathcal{I}_{\epsilon_{\omega_k}}|/\alpha_d^2$ is plotted for two outgoing null detectors in a (1+1) dimensional DeSitter spacetime with respect to the dimensionless frequency of the field $\bar{\omega}_k$ for fixed $\Delta\bar{E} = 1$, and $d/\alpha_d = 1$.

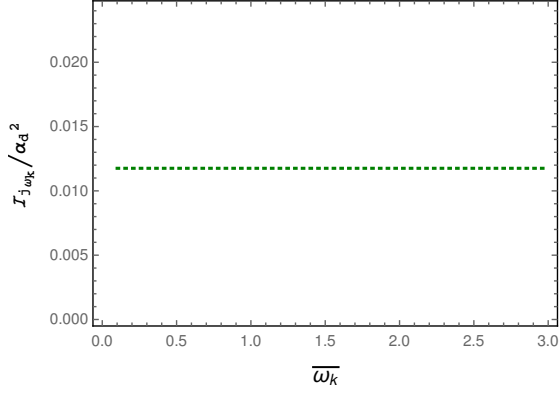


FIG. 17: The quantity $\mathcal{I}_{j_{\omega_k}}/\alpha_d^2$, signifying the concurrence, is plotted for two outgoing null detectors in a (1+1) dimensional DeSitter spacetime with respect to the dimensionless frequency of the field $\bar{\omega}_k$ for fixed $\Delta\bar{E} = 1$, and $d/\alpha_d = 1$.

$$= \int_{-\infty}^{\infty} dt_B \int_{-\infty}^{\infty} dt_A e^{i(\Delta E^A t_A + \Delta E^B t_B)} \times \left[e^{i\omega_k d} + e^{-i\omega_k d} e^{2i\omega_k \alpha_d (e^{-t_B/\alpha_d} - e^{-t_A/\alpha_d})} \right]. \quad (65)$$

Here also one can observe that the integration over the first quantity with $e^{i\omega_k d}$ as multiplicative factor will provide the multiplication of Dirac delta distributions $\delta(\Delta E^A)$ and $\delta(\Delta E^B)$. Therefore that part of the integral will vanish as the detector transition energy $\Delta E^j > 0$. Now with the change of variables $z_j = e^{-t_j/\alpha_d}$ one simplifies the previous integral as

$$\mathcal{I}_{\epsilon_{\omega_k}}^W = \alpha_d^2 e^{-i\omega_k d} \int_0^{\infty} dz_A \int_0^{\infty} dz_B e^{2i\omega_k \alpha_d (z_B - z_A)} \times z_A^{-i\Delta E^A \alpha_d - 1} z_B^{-i\Delta E^B \alpha_d - 1}. \quad (66)$$

By introducing regulators of the form $(z_A z_B)^\epsilon e^{-\epsilon(z_A + z_B)}$, with a positive real parameter ϵ , one can evaluate this integral. The explicit expression

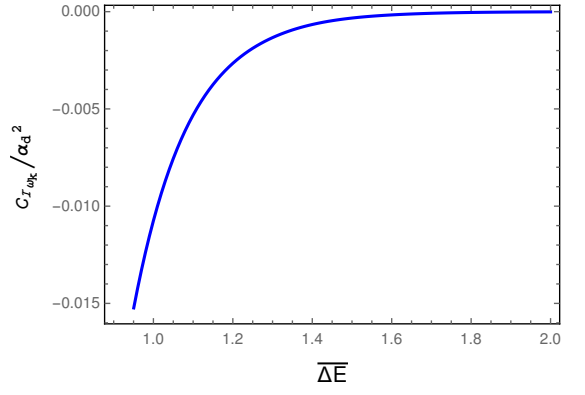


FIG. 18: The quantity $\mathcal{C}_{\mathcal{I}_{\omega_k}}/\alpha_d^2$, signifying the concurrence, is plotted for two outgoing null detectors in a (1+1) dimensional DeSitter spacetime with respect to the dimensionless transition energy $\Delta\bar{E}$ of the detectors for fixed dimensionless frequency of the field $\bar{\omega}_k = 0.2$, and $d = 0$.

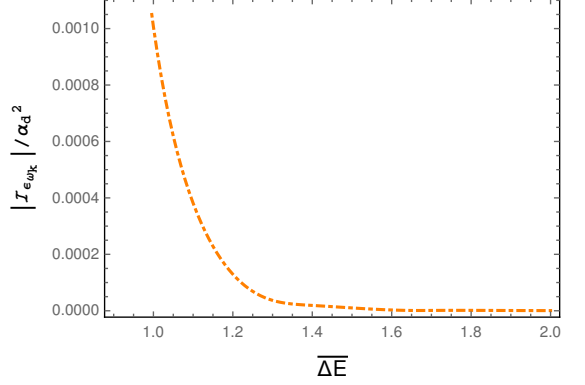


FIG. 19: The quantity $|\mathcal{I}_{\epsilon_{\omega_k}}|/\alpha_d^2$ is plotted for two outgoing null detectors in a (1+1) dimensional DeSitter spacetime with respect to the dimensionless transition energy $\Delta\bar{E}$ of the detectors for fixed dimensionless frequency of the field $\bar{\omega}_k = 0.2$, and $d = 0$.

after the integration is carried out, is provided in the Appendix. C 1. We now proceed to evaluate the integral $\mathcal{I}_{\epsilon_{\omega_k}}^R$, which can be expressed as

$$\begin{aligned} \mathcal{I}_{\epsilon_{\omega_k}}^R &= \int_{-\infty}^{\infty} dt_B \int_{-\infty}^{\infty} dt_A e^{i(\Delta E^A t_A + \Delta E^B t_B)} \theta(\eta_A - \eta_B) \\ &\times \left\{ e^{-i\omega_k(u_A - u_B)} + e^{-i\omega_k(v_A - v_B)} \right. \\ &\quad \left. - e^{-i\omega_k(u_B - u_A)} - e^{-i\omega_k(v_B - v_A)} \right\} \\ &= \alpha_d^2 \int_0^{\infty} dz_A \int_{z_A}^{\infty} dz_B z_A^{-i\Delta E^A \alpha_d - 1} z_B^{-i\Delta E^B \alpha_d - 1} \\ &\times \left\{ e^{i\omega_k d} e^{2i\omega_k \alpha_d (z_A - z_B)} - e^{-i\omega_k d} e^{2i\omega_k \alpha_d (z_B - z_A)} \right. \\ &\quad \left. - 2i \sin \omega_k d \right\}. \quad (67) \end{aligned}$$

In de Sitter background, the real scalar field is decomposed with respect to the positive and negative frequency

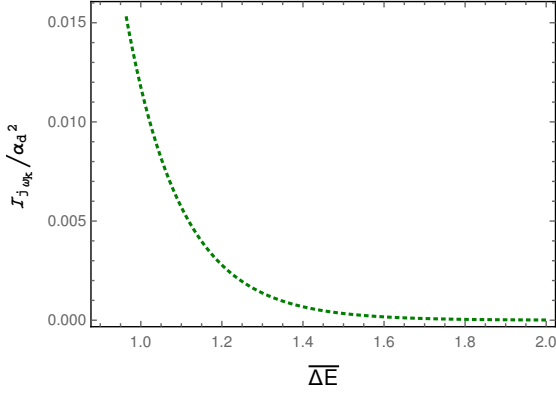


FIG. 20: The quantity $\mathcal{I}_{j\omega_k}/\alpha_d^2$ is plotted for two outgoing null detectors in a $(1+1)$ dimensional DeSitter spacetime with respect to the dimensionless transition energy $\overline{\Delta E}$ of the detectors for fixed dimensionless frequency of the field $\bar{\omega}_k = 0.2$, and $d = 0$.

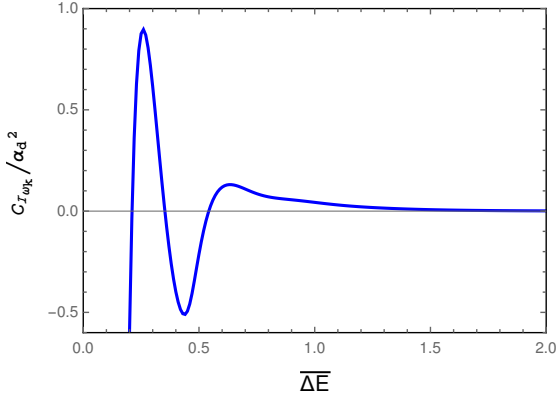


FIG. 21: The quantity $\mathcal{C}_{\mathcal{I}\omega_k}/\alpha_d^2$, signifying the concurrence, is plotted for two outgoing null detectors in a $(1+1)$ dimensional DeSitter spacetime with respect to the dimensionless transition energy $\overline{\Delta E}$ of the detectors for fixed dimensionless frequency of the field $\bar{\omega}_k = 0.2$, and $d/\alpha_d = 1$.

modes, represented in the conformal time η . Therefore, the time T_j inside the Heaviside step function here is denoted by the conformal time. Here for positive α_d one obtains $\theta(\eta_A - \eta_B) = \theta(t_A - t_B) = \theta(z_B - z_A)$ using the relation (21), and we have used this fact to realize the previous expression. We also mention that utilization of the function $\theta(z_B - z_A)$ transformed the z_B integration range from $[0, \infty)$ to $[z_A, \infty)$ in the representation of Eq. (67). This integral can be evaluated numerically with the introduction of the regulator of the form $(z_A z_B)^\epsilon e^{-\epsilon(z_A + z_B)}$, with positive real ϵ .

In Fig. 12 we have plotted the dimensionless quantity $\mathcal{C}_{\mathcal{I}\omega_k}/\alpha_d^2$, representing the concurrence corresponding to a specific field mode frequency ω_k , with respect to the dimensionless parameter $\bar{\omega}_k = \omega_k \alpha_d$ for fixed $\overline{\Delta E^A} = \alpha_d \Delta E^A = 1$, $\overline{\Delta E^B} = \alpha_d \Delta E^B = 1$, and $d = 0$. This plot asserts that in this parameter range entanglement harvesting is not possible from the conformal vacuum us-

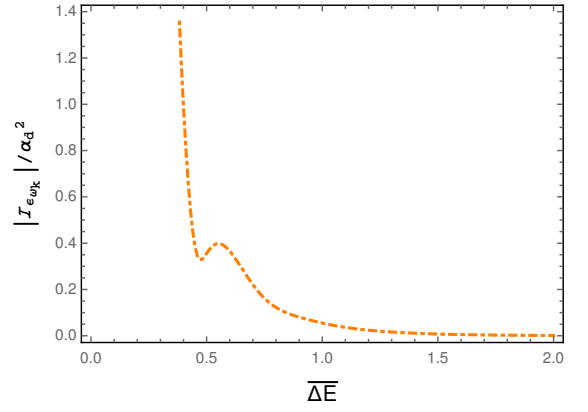


FIG. 22: The quantity $|\mathcal{I}_{\varepsilon\omega_k}|/\alpha_d^2$ is plotted for two outgoing null detectors in a $(1+1)$ dimensional DeSitter spacetime with respect to the dimensionless transition energy $\overline{\Delta E}$ of the detectors for fixed dimensionless frequency of the field $\bar{\omega}_k = 0.2$, and $d/\alpha_d = 1$.

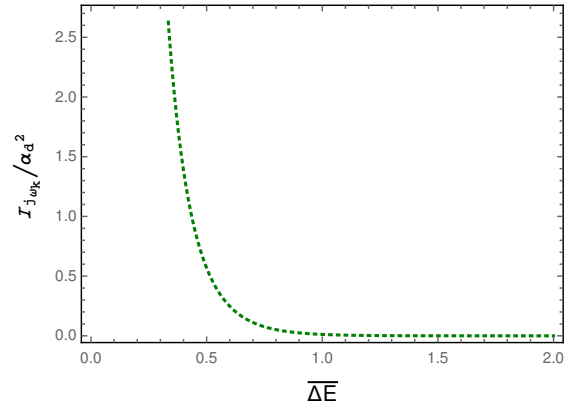


FIG. 23: The quantity $\mathcal{I}_{j\omega_k}/\alpha_d^2$ is plotted for two outgoing null detectors in a $(1+1)$ dimensional DeSitter spacetime with respect to the dimensionless transition energy $\overline{\Delta E}$ of the detectors for fixed dimensionless frequency of the field $\bar{\omega}_k = 0.2$, and $d/\alpha_d = 1$.

ing the outgoing null detectors in de Sitter spacetime. We observed that here $\mathcal{I}_{j\omega_k}$ is larger than $|\mathcal{I}_{\varepsilon\omega_k}|$ from Fig. 13 and 14, which results in the negative $(|\mathcal{I}_\varepsilon| - \sqrt{\mathcal{I}_A \mathcal{I}_B})/\alpha_d^2$. However, from Fig. 15 with respect to the same parameters but $d/\alpha_d = 1$ we observed that the quantity $\mathcal{C}_{\mathcal{I}\omega_k}/r_H^2$ is now positive making entanglement harvesting possible in this scenario. From Fig. 16 and 17 we see that now $\mathcal{I}_{j\omega_k}$ is smaller than $|\mathcal{I}_{\varepsilon\omega_k}|$. From Fig. 14 and 17 one can observe that the quantity $\mathcal{I}_{j\omega_k}$ involving individual detector transition probabilities is independent of $\bar{\omega}_k$, which is also confirmed from Eq. (63).

We have plotted $\mathcal{C}_{\mathcal{I}\omega_k}/\alpha_d^2$ with respect to the dimensionless transition energy $\overline{\Delta E}$ of the detectors for fixed $\bar{\omega}_k = 1$ and $d = 0$ in Fig. 18. This plot also states that in this parameter range the entanglement harvesting is not possible and Fig. 19 and 20 support this claim. However, from Fig. 21 with 22 and 23, where the similar plots are

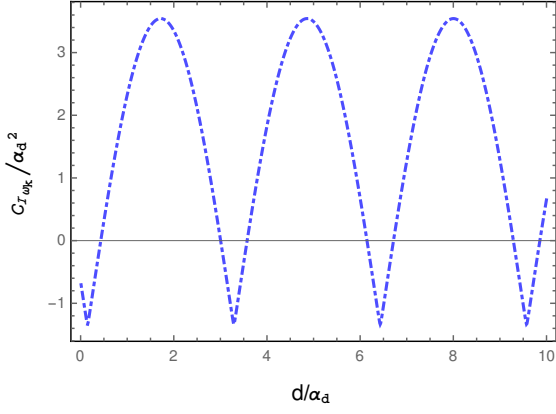


FIG. 24: The quantity $\mathcal{C}_{\mathcal{I}_{\omega_k}}/\alpha_d^2$ is plotted for two outgoing null detectors in different parallel paths in a (1 + 1) dimensional de-Sitter spacetime with respect to the separation between the two paths d/α_d . The frequency of the field and the detector transition energies are fixed at $\bar{\omega}_k = 0.4$ and $\bar{\Delta E} = 1$.

obtained for $d/\alpha_d = 1$, we observed that entanglement harvesting is possible in certain discrete ranges of $\bar{\Delta E}$.

In Fig. 24 we have plotted the concurrence denoting quantity $\mathcal{C}_{\mathcal{I}_{\omega_k}}/\alpha_d^2$ with respect to the dimensionless distance d/α_d between the two detectors' null trajectories for fixed $\bar{\Delta E} = 1$ and $\bar{\omega}_k = 0.4$. This plot is consistent with the findings of Fig. 12 and Fig. 18, reconfirming that for $d/\alpha_d = 0$ harvesting is not possible. Fig. 24 indicates that like the Schwarzschild case here also harvesting is periodic with respect to d/α_d , but unlike an entanglement shadow points from the Schwarzschild case here we get periodic shadow regions of d/α_d where entanglement harvesting is not possible, e.g., when d/α_d seems to be between 3 and 3.5.

2. (1+3)-dimensions

In (1 + 3)-dimensional de Sitter spacetime one can express the integrals from Eq. (4), essential for perceiving the entanglement harvesting (7), as

$$\begin{aligned} \mathcal{I}_j &= \int_{-\infty}^{\infty} dt'_j \int_{-\infty}^{\infty} dt_j e^{-i\Delta E^j(t'_j - t_j)} G_D^+(X'_j, X_j) \\ &= \int \frac{d^2 k_{\perp}}{(2\pi)^2 2\omega_k} \int_0^{\infty} dk_x \mathcal{I}_{j\omega_k}, \end{aligned} \quad (68)$$

where, $\omega_k^2 = k_{\perp}^2 + k_x^2$, and $k_{\perp}^2 = k_y^2 + k_z^2$. These integrations over t'_j , and t_j can be solved for detectors in outgoing null paths using the Green's functions (40) as

$$\begin{aligned} \mathcal{I}_{j\omega_k} &= \int_{-\infty}^{\infty} dt'_j \int_{-\infty}^{\infty} dt_j \frac{e^{-i\Delta E^j(t'_j - t_j)}}{a(\eta'_j)a(\eta_j)} \\ &\times \left[e^{ik_x \Delta x_{j'j} - i\omega_k \Delta \eta_{j'j}} + e^{-ik_x \Delta x_{j'j} - i\omega_k \Delta \eta_{j'j}} \right] \end{aligned}$$

$$\begin{aligned} &= \int_{-\infty}^{\infty} dt'_j \int_{-\infty}^{\infty} dt_j e^{-i\Delta E^j(t'_j - t_j)} \\ &\times \frac{1}{e^{t'_j/\alpha_d + t_j/\alpha_d}} \left[e^{i\alpha_d(\omega_k - k_x)(e^{-t'_j/\alpha_d} - e^{-t_j/\alpha_d})} \right. \\ &\quad \left. + e^{i\alpha_d(\omega_k + k_x)(e^{-t'_j/\alpha_d} - e^{-t_j/\alpha_d})} \right]. \end{aligned} \quad (69)$$

With the change of variables $z_j = e^{-t_j/\alpha_d}$ this expression changes into

$$\begin{aligned} \mathcal{I}_{j\omega_k} &= \alpha_d^2 \left[\left| \int_0^{\infty} dz_j z_j^{-i\alpha_d \Delta E^j} e^{-i\alpha_d(\omega_k - k_x)z_j} \right|^2 \right. \\ &\quad \left. + \left| \int_0^{\infty} dz_j z_j^{-i\alpha_d \Delta E^j} e^{-i\alpha_d(\omega_k + k_x)z_j} \right|^2 \right]. \end{aligned} \quad (70)$$

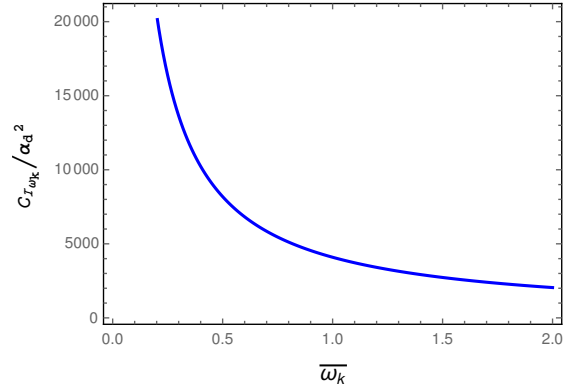


FIG. 25: The quantity $\mathcal{C}_{\mathcal{I}_{\omega_k}}/\alpha_d^2$, signifying the concurrence, is plotted for two outgoing null detectors in a (1 + 3) dimensional DeSitter spacetime with respect to the dimensionless frequency of the field $\bar{\omega}_k = \omega_k \alpha_d$ for fixed dimensionless detector transition energy $\bar{\Delta E} = \Delta E \alpha_d = 1$, and $d/\alpha_d = 0$. We considered $\bar{k}_x = \alpha_d k_x = \bar{\omega}_k/2$.

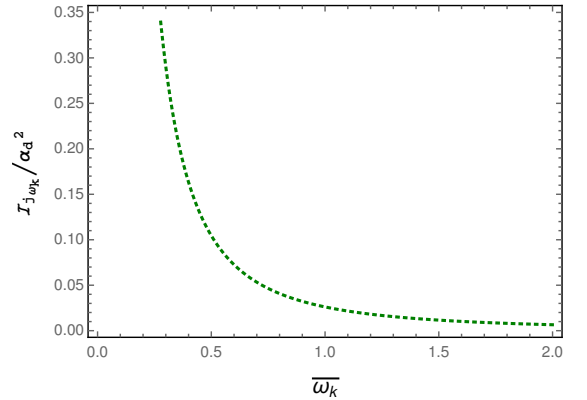


FIG. 26: The quantity $\mathcal{I}_{j\omega_k}/\alpha_d^2$, signifying the concurrence, is plotted for two outgoing null detectors in a (1 + 3) dimensional DeSitter spacetime with respect to the dimensionless frequency of the field $\bar{\omega}_k = \omega_k \alpha_d$ for fixed $\bar{\Delta E} = 1$, and $d/\alpha_d = 0$. We considered $\bar{k}_x = \bar{\omega}_k/2$.

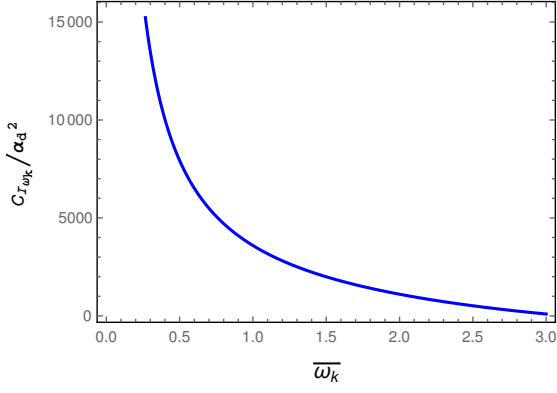


FIG. 27: The quantity $\mathcal{C}_{\mathcal{I}_{\omega_k}}/\alpha_d^2$, signifying the concurrence, is plotted for two outgoing null detectors in a (1 + 3) dimensional DeSitter spacetime with respect to the dimensionless frequency of the field $\bar{\omega}_k = \omega_k \alpha_d$ for fixed dimensionless detector transition energy $\Delta\bar{E} = \Delta E \alpha_d = 1$, and $d/\alpha_d = 1$. We considered $\bar{k}_x = \bar{\omega}_k/2$.

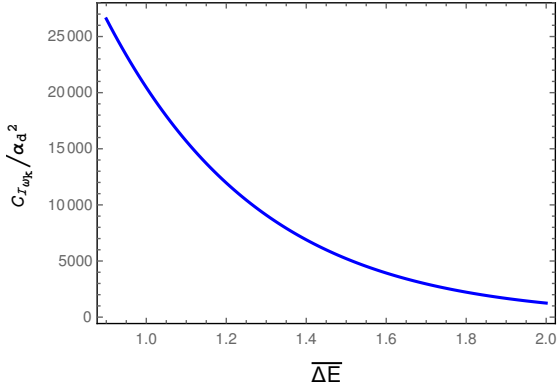


FIG. 28: The quantity $\mathcal{C}_{\mathcal{I}_{\omega_k}}/\alpha_d^2$, signifying the concurrence, is plotted for two outgoing null detectors in a (1 + 3) dimensional DeSitter spacetime with respect to the dimensionless transition energy $\Delta\bar{E}$ of the detectors for fixed dimensionless frequency of the field $\bar{\omega}_k = 0.2$, $\bar{k}_x = \bar{\omega}_k/2$, and $d/\alpha_d = 0$.

These integrals can be performed using regulators of the form $(z^\epsilon e^{-\epsilon z})$, and in the limit $\epsilon \rightarrow 0$ results in

$$\mathcal{I}_{j\omega_k} = \left[\frac{1}{(\omega_k - k_x)^2} + \frac{1}{(\omega_k + k_x)^2} \right] \pi \alpha_d \Delta E^j \times \frac{1}{e^{2\pi\alpha_d \Delta E^j} - 1}. \quad (71)$$

Now one can proceed to evaluate the value of \mathcal{I}_ϵ in a similar manner. In particular \mathcal{I}_ϵ can be expressed as

$$\mathcal{I}_\epsilon = - \int \frac{d^2 k_\perp}{(2\pi)^2 2\omega_k} \int_0^\infty dk_x \left[\mathcal{I}_{\epsilon\omega_k}^W + \mathcal{I}_{\epsilon\omega_k}^R \right]. \quad (72)$$

Here the first integral $\mathcal{I}_{\epsilon\omega_k}^W$, which has emerged due to the Wightman function, is

$$\mathcal{I}_{\epsilon\omega_k}^W = \int_{-\infty}^\infty dt_B \int_{-\infty}^\infty dt_A e^{i(\Delta E^A t_A + \Delta E^B t_B)} \frac{1}{a(\eta_A)a(\eta_B)}$$

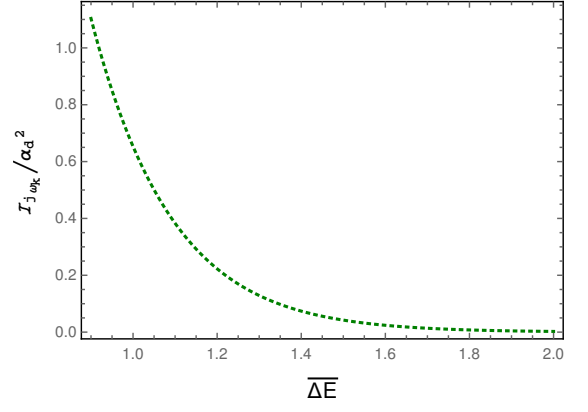


FIG. 29: The quantity $\mathcal{I}_{j\omega_k}/\alpha_d^2$ is plotted for two outgoing null detectors in a (1 + 3) dimensional DeSitter spacetime with respect to the dimensionless transition energy $\Delta\bar{E}$ of the detectors for fixed dimensionless frequency of the field $\bar{\omega}_k = 0.2$, $\bar{k}_x = \bar{\omega}_k/2$, and $d/\alpha_d = 0$.

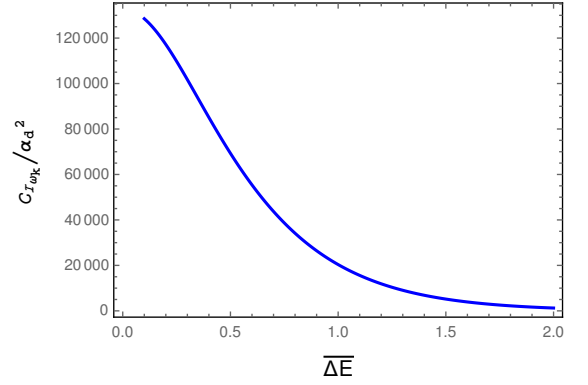


FIG. 30: The quantity $\mathcal{C}_{\mathcal{I}_{\omega_k}}/\alpha_d^2$, signifying the concurrence, is plotted for two outgoing null detectors in a (1 + 3) dimensional DeSitter spacetime with respect to the dimensionless transition energy $\Delta\bar{E}$ of the detectors for fixed dimensionless frequency of the field $\bar{\omega}_k = 0.2$, $\bar{k}_x = \bar{\omega}_k/2$, and $d/\alpha_d = 1$.

$$\times \left[e^{ik_x \Delta x_{BA} - i\omega_k \Delta \eta_{BA}} + e^{-ik_x \Delta x_{BA} - i\omega_k \Delta \eta_{BA}} \right]. \quad (73)$$

With a this integral turns into

$$\mathcal{I}_{\epsilon\omega_k}^W = \alpha_d^2 \int_0^\infty dz_B \int_0^\infty dz_A z_B^{-i\alpha_d \Delta E^B} z_A^{-i\alpha_d \Delta E^A} \times \left[e^{i\alpha_d(\omega_k - k_x)(z_B - z_A)} e^{ik_x d} + e^{i\alpha_d(\omega_k + k_x)(z_B - z_A)} e^{-ik_x d} \right]. \quad (74)$$

This integral can be straightforwardly evaluated with the introduction of the regulator $(z_A z_B)^\epsilon e^{-\epsilon(z_A + z_B)}$. We mention that the other integral $\mathcal{I}_{\epsilon\omega_k}^R$, arriving from the retarded Green's function, can also be provided a final form in a similar manner after the change of variables as

$$\mathcal{I}_{\epsilon\omega_k}^R = \alpha_d^2 \int_0^\infty dz_A \int_{z_A}^\infty dz_B z_B^{-i\alpha_d \Delta E^B} z_A^{-i\alpha_d \Delta E^A}$$

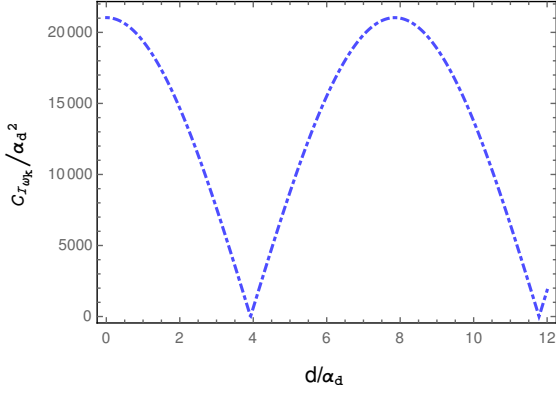


FIG. 31: The quantity $\mathcal{C}_{\mathcal{I}_{\omega_k}}/\alpha_d^2$ is plotted for two outgoing null detectors in different parallel paths in a (1 + 3) dimensional de-Sitter spacetime with respect to the separation between the two paths d/α_d . The frequency of the field and the detector transition energies are fixed at $\bar{\omega}_k = 0.4$, $\bar{k}_x = \bar{\omega}_k/2$, and $\overline{\Delta E} = 1$.

$$\begin{aligned} & \times \left[e^{i\alpha_d(\omega_k - k_x)(z_A - z_B)} e^{-ik_x d} \right. \\ & + e^{i\alpha_d(\omega_k + k_x)(z_A - z_B)} e^{ik_x d} \\ & - e^{i\alpha_d(\omega_k - k_x)(z_B - z_A)} e^{ik_x d} \\ & \left. - e^{i\alpha_d(\omega_k + k_x)(z_B - z_A)} e^{-ik_x d} \right], \quad (75) \end{aligned}$$

which can also be evaluated in a similar manner introducing a regulator same as the one in the previous case, see Appendix C 2.

In a (1 + 3) dimensional de Sitter spacetime we have plotted $\mathcal{C}_{\mathcal{I}_{\omega_k}}/\alpha_d^2$, representing the concurrence, in Fig. 25 with respect to the dimensionless parameter $\bar{\omega}_k$ for $d/\alpha_d = 0$ and $\overline{\Delta E^A} = 1 = \overline{\Delta E^B}$. While in Fig. 26 we have represented the individual detector transition probability with respect to $\bar{\omega}_k$ for the same set of parameters. Furthermore, for $d/\alpha_d = 1$ and $\overline{\Delta E} = 1$ we have plotted $\mathcal{C}_{\mathcal{I}_{\omega_k}}/\alpha_d^2$ in Fig. 27 with respect to the parameter $\bar{\omega}_k$. Both of these plots suggest the possibility of entanglement harvesting and they are not qualitatively different either. They suggest that entanglement harvesting decreases with increasing field mode frequency. On the other hand, in Fig. 28 we have depicted the concu-

rence with respect to the dimensionless transition energy $\overline{\Delta E}$ for $d/\alpha_d = 0$ and fixed $\bar{\omega}_k = 1$. While the individual detector transition probability is depicted in Fig. 29. Moreover, for $d/\alpha_d = 1$ and for the same other parameters we have depicted the concurrence in Fig. 30. These figures also predict the possibility of entanglement harvesting for the considered parameter range, and states that entanglement harvesting decreases with increasing detector transition energy. It should be noted that unlike the (1 + 1) dimensional case in (1 + 3) dimensions entanglement harvesting is possible for $d/\alpha_d = 0$ in similar parameter range.

In Fig. 31 we have portrayed the concurrence with respect to the dimensionless distance d/α_d between the two detectors' null trajectories for fixed $\overline{\Delta E} = 1$ and $\bar{\omega}_k = 0.4$. Like the previous Schwarzschild and (1 + 1) dimensional de Sitter cases this plot shows a periodicity of obtained concurrence with respect to d/α_d . However, this plot is more like the Schwarzschild case than the (1 + 1) dimensional de Sitter case as one periodically reaches to entanglement shadow points (points of vanishing harvesting) rather than shadow regions (regions of zero harvesting).

VII. MUTUAL INFORMATION

A. In Schwarzschild spacetime with respect to the Boulware and Unruh vacuum

To talk about mutual information of two outgoing null detectors in a Schwarzschild black hole spacetime one needs to evaluate the value of the quantity P_{AB} , thus the integral \mathcal{I}_{AB} . One can express this integral as

$$\begin{aligned} \mathcal{I}_{AB} &= \int_{-\infty}^{\infty} d\tau_B \int_{-\infty}^{\infty} d\tau_A e^{-i(\Delta E^B \tau_B - \Delta E^A \tau_A)} G_W(X_B, X_A) \\ &= \int_0^{\infty} \frac{d\omega_k}{4\pi\omega_k} \mathcal{I}_{AB\omega_k}. \quad (76) \end{aligned}$$

Now we shall be evaluating $\mathcal{I}_{AB\omega_k}$ corresponding to a certain field mode frequency ω_k . In particular considering field mode decomposition corresponding to the Boulware vacuum one can get

$$\begin{aligned} \mathcal{I}_{AB\omega_k} &= \int_{-\infty}^{\infty} d\tau_B \int_{-\infty}^{\infty} d\tau_A e^{-i(\Delta E^B \tau_B - \Delta E^A \tau_A)} \left[e^{i\omega_k d} + e^{-i\omega_k(2r_B - 2r_A - d)} \left(\frac{r_B - r_H}{r_A - r_H} \right)^{-2i\omega_k r_H} \right] \\ &= r_H^2 e^{i(\Delta E^A + \omega_k)d + i(\Delta E^A - \Delta E^B)r_H} \int_0^{\infty} dy_B \frac{y_B + 2}{y_B} \int_0^{\infty} dy_A \frac{y_A + 2}{y_A} \\ & \quad e^{i(\Delta E^A y_A - \Delta E^B y_B)r_H} y_A^{2i\Delta E^A r_H} y_B^{-2i\Delta E^B r_H} \left[1 + e^{-2i\omega_k r_H(y_B - y_A)} \left(\frac{y_B}{y_A} \right)^{-2i\omega_k r_H} \right]. \quad (77) \end{aligned}$$

On the other hand, considering field mode decomposition corresponding to the Unruh vacuum one gets

$$\begin{aligned} \mathcal{I}_{AB\omega_k} &= \int_{-\infty}^{\infty} d\tau_B \int_{-\infty}^{\infty} d\tau_A e^{-i(\Delta E^B \tau_B - \Delta E^A \tau_A)} \left[\exp \left\{ i\omega_k 2r_H \left(1 - e^{-\frac{d}{2r_H}} \right) \right\} + e^{-i\omega_k(2r_B - 2r_A - d)} \left(\frac{r_B - r_H}{r_A - r_H} \right)^{-2i\omega_k r_H} \right] \\ &= r_H^2 e^{i\Delta E^A d + i(\Delta E^A - \Delta E^B)r_H} \int_0^{\infty} dy_B \frac{y_B + 2}{y_B} \int_0^{\infty} dy_A \frac{y_A + 2}{y_A} e^{i(\Delta E^A y_A - \Delta E^B y_B)r_H} \\ &\quad y_A^{2i\Delta E^A r_H} y_B^{-2i\Delta E^B r_H} \left[\exp \left\{ i\omega_k 2r_H \left(1 - e^{-\frac{d}{2r_H}} \right) \right\} + e^{i\omega_k d} e^{-2i\omega_k r_H(y_B - y_A)} \left(\frac{y_B}{y_A} \right)^{-2i\omega_k r_H} \right]. \end{aligned} \quad (78)$$

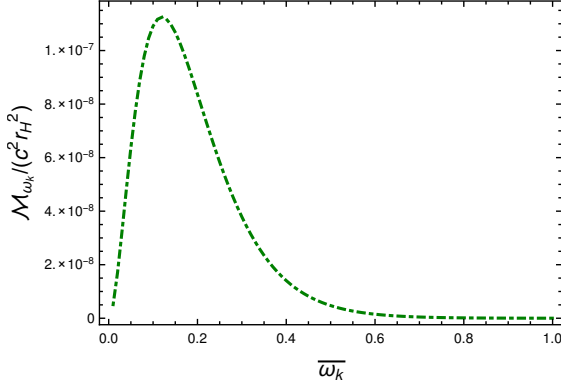


FIG. 32: The mutual information $\mathcal{M}_{\omega_k}(\rho_{AB})/(c^2 r_H^2)$ perceived by two out going null detectors corresponding to the Boulware and Unruh vacuum in plotted with respect to the dimensionless frequency of the field modes $\bar{\omega}_k = r_H \omega_k$ for fixed transition frequency $\bar{\Delta E} = r_H \Delta E = 1$.

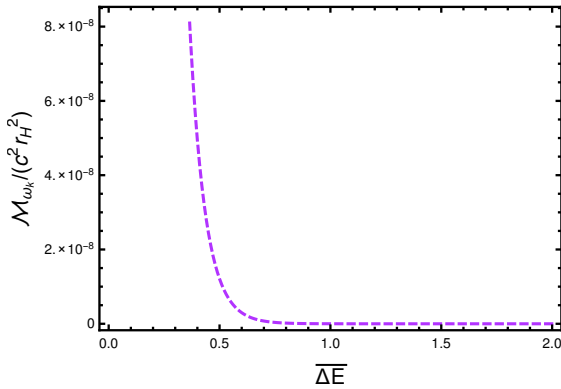


FIG. 33: The mutual information $\mathcal{M}_{\omega_k}(\rho_{AB})/(c^2 r_H^2)$ perceived by two out going null detectors corresponding to the Boulware and Unruh vacuum in plotted with respect to the dimensionless transition frequency $\bar{\Delta E} = r_H \Delta E$ for fixed dimensionless field mode frequency $\bar{\omega}_k = r_H \omega_k = 1$.

One should notice that the first terms in the square brackets on the right hand side of Eq. (77) and (78) vanishes and when $\Delta E^A = \Delta E^B = \Delta E$ both of these integrals get significantly simplified and can be evaluated to be

$$\mathcal{I}_{AB\omega_k} = e^{i(\Delta E^A + \omega_k)d} \frac{4\pi r_H \omega_k^2}{(\Delta E + \omega_k)(\Delta E + 2\omega_k)^2}$$

$$\times \frac{1}{e^{4\pi r_H(\Delta E + \omega_k)} - 1}, \quad (79)$$

which is same as $\mathcal{I}_{j\omega_k}$ up-to a phase factor for equal detector transition energies. Now it should be mentioned that unlike the expression of the concurrence, the mutual information has multiple disparate multiplicative expectation values of the monopole moment operators $m_j(0)$. In that case one cannot take a common factor of them out from the expression of the mutual information. In particular, from the operator form of $m_j(0) = |E_1^j\rangle\langle E_0^j| + |E_0^j\rangle\langle E_1^j|$ one can get the expectation values $\langle E_1^j | m_j(0) | E_0^j \rangle = 1$. In that case $P_{A\omega_k} = \mathcal{I}_{A\omega_k}$, $P_{B\omega_k} = \mathcal{I}_{B\omega_k}$, and $P_{AB\omega_k} = \mathcal{I}_{AB\omega_k}$, where $P_j = \int_{-\infty}^{\infty} dk / (4\pi\omega_k) P_{j\omega_k}$. For $\Delta E^A = \Delta E^B = \Delta E$, let us consider $\mathcal{I}_{A\omega_k} = \mathcal{I}_{B\omega_k} = |\mathcal{I}_{AB\omega_k}| = \mathcal{I}_{\omega_k}$. Then $P_{+\omega_k} = \mathcal{I}_{\omega_k}$ and $P_{-\omega_k} = 0$, and one can get the mutual information for fixed field frequency ω_k as

$$\mathcal{M}_{\omega_k}(\rho_{AB}) = c^2 2 \mathcal{I}_{\omega_k} \ln 2 + \mathcal{O}(c^4). \quad (80)$$

Therefore we have observed that in both the Boulware and Unruh vacuum cases the mutual information corresponding to a certain field mode frequency upto $\mathcal{O}(c^2)$ are the same and independent of the distance d , between different outgoing null paths. Since mutual information is independent of d and non-vanishing, the correlation is classical at the values of d where entanglement harvesting does not occur. In Fig. 32 and 33 we have plotted the dimensionless mutual information $\mathcal{M}_{\omega_k}(\rho_{AB})/(c^2 r_H^2)$ with respect to the dimensionless parameters $\bar{\omega}_k$ and $\bar{\Delta E}$ respectively. It is observed that the mutual information decreases with increasing detector transition energy.

B. de Sitter universe

1. (1+1)-dimensions

Now we proceed to talk about the mutual information of two outgoing null detectors in a de Sitter background. Again we express the integral $\mathcal{I}_{AB} = \int_0^{\infty} d\omega_k / (4\pi\omega_k) \mathcal{I}_{AB\omega_k}$ to evaluate P_{AB} . Furthermore, this integral $\mathcal{I}_{AB\omega_k}$ corresponding to the de Sitter vacuum is

$$\mathcal{I}_{AB\omega_k} = \int_{-\infty}^{\infty} d\tau_B \int_{-\infty}^{\infty} d\tau_A e^{-i(\Delta E^B \tau_B - \Delta E^A \tau_A)}$$

$$\left[e^{i\omega_k d} + e^{-i\omega_k d} e^{-2i\omega_k \alpha_d (e^{-t_A/\alpha_d} - e^{-t_B/\alpha_d})} \right]. \quad (81)$$

Like the previous cases here also the integration over $e^{i\omega_k d}$ vanishes using the properties of the Dirac delta distribution for $\Delta E^j > 0$. Then with the change of variables $e^{-t_j/\alpha_d} = z_j$ the integral $\mathcal{I}_{AB\omega_k}$ becomes

$$\mathcal{I}_{AB\omega_k} = e^{-i\omega_k d} \alpha_d^2 \int_0^\infty dz_B \int_0^\infty dz_A e^{-2i\omega_k \alpha_d (z_A - z_B)} \times z_A^{-i\alpha_d \Delta E^A - 1} z_B^{i\alpha_d \Delta E^B - 1}. \quad (82)$$

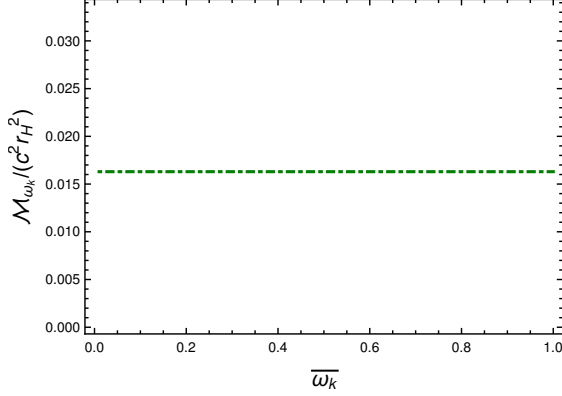


FIG. 34: The mutual information $\mathcal{M}_{\omega_k}(\rho_{AB})/(c^2 \alpha_d^2)$ in (1+1) dimensional de Sitter spacetime as perceived by two out going null detectors is plotted with respect to the dimensionless frequency of the field modes $\bar{\omega}_k = \alpha_d \omega_k$ for fixed transition frequency $\Delta \bar{E} = \alpha_d \Delta E = 1$, and $d/\alpha_d = 0$.

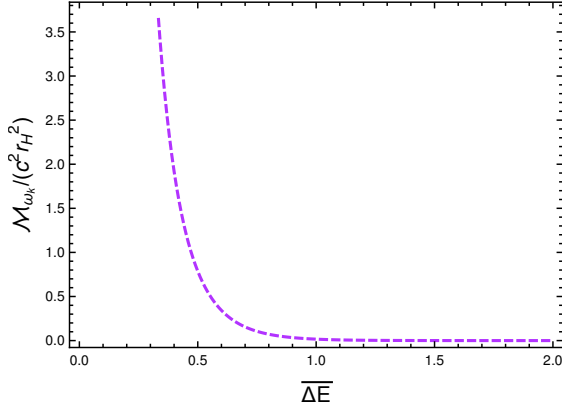


FIG. 35: The mutual information $\mathcal{M}_{\omega_k}(\rho_{AB})/(c^2 r_H^2)$ in (1+1) dimensional de Sitter spacetime as perceived by two out going null detectors is plotted with respect to the dimensionless transition frequency $\Delta \bar{E} = r_H \Delta E$ for fixed dimensionless field mode frequency $\bar{\omega}_k = r_H \omega_k = 1$, and $d/\alpha_d = 0$.

When $\Delta E^A = \Delta E^B = \Delta E$ this integral gets significantly simplified and is evaluated to be

$$\mathcal{I}_{AB\omega_k} = e^{-i\omega_k d} \frac{2\pi\alpha_d}{\Delta E} \frac{1}{e^{2\pi\alpha_d \Delta E} - 1}, \quad (83)$$

which is same as $\mathcal{I}_{j\omega_k}$ up-to a phase factor. In that case one cannot take a common factor of them out from the expression of the mutual information. With the consideration of the form of the monopole moment operator $m_j(0) = |E_1^j\rangle\langle E_0^j| + |E_0^j\rangle\langle E_1^j|$ one gets the expectation values $\langle E_1^j | m_j(0) | E_0^j \rangle = 1$. In that case $P_{A\omega_k} = \mathcal{I}_{A\omega_k}$, $P_{B\omega_k} = \mathcal{I}_{B\omega_k}$, and $P_{AB\omega_k} = \mathcal{I}_{AB\omega_k}$, where $P_j = \int_{-\infty}^\infty dk / (4\pi\omega_k) P_{j\omega_k}$. For $\Delta E^A = \Delta E^B = \Delta E$, we further consider $\mathcal{I}_{A\omega_k} = \mathcal{I}_{B\omega_k} = |\mathcal{I}_{AB\omega_k}| = \mathcal{I}_{\omega_k}$. Then $P_{+\omega_k} = \mathcal{I}_{\omega_k}$ and $P_{-\omega_k} = 0$, and one can get the mutual information for a certain field frequency ω_k as

$$\mathcal{M}_{\omega_k}(\rho_{AB}) = c^2 2 \mathcal{I}_{\omega_k} \ln 2 + \mathcal{O}(c^4). \quad (84)$$

We observe that this mutual information is independent of the distance d , between different outgoing null paths, and the field mode frequency ω_k , see (63) for \mathcal{I}_{ω_k} . The Mutual information $\mathcal{M}_{\omega_k}(\rho_{AB})/(c^2 r_H^2)$ in this scenario is plotted as functions of $\bar{\omega}_k$ and $\Delta \bar{E}$ respectively in Fig. 34 and 35. From these figures one asserts that mutual information decreases with increasing detector transition energy.

2. (1+3)-dimensions

We are going to evaluate the integral \mathcal{I}_{AB} for the estimation of the quantity P_{AB} . This integral can be further expressed as

$$\begin{aligned} \mathcal{I}_{AB} &= \int_{-\infty}^\infty d\tau_B \int_{-\infty}^\infty d\tau_A e^{-i(\Delta E^B \tau_B - \Delta E^A \tau_A)} G_W(X_B, X_A) \\ &= \int \frac{d^2 k_\perp}{(2\pi)^2 2\omega_k} \int_0^\infty dk_x \mathcal{I}_{AB\omega_k}. \end{aligned} \quad (85)$$

We are now going to evaluate the integral $\mathcal{I}_{AB\omega_k}$ in (1+3) dimensions corresponding to the conformal vacuum as

$$\begin{aligned} \mathcal{I}_{AB\omega_k} &= \int_{-\infty}^\infty d\tau_B \int_{-\infty}^\infty d\tau_A e^{-i(\Delta E^B \tau_B - \Delta E^A \tau_A)} e^{-\frac{t_B + t_A}{\alpha_d}} \\ &\quad \left[e^{ik_x d} e^{i\alpha_d(\omega_k - k_x)(e^{-t_B/\alpha_d} - e^{-t_A/\alpha_d})} \right. \\ &\quad \left. + e^{-ik_x d} e^{i\alpha_d(\omega_k + k_x)(e^{-t_B/\alpha_d} - e^{-t_A/\alpha_d})} \right]. \end{aligned} \quad (86)$$

Now one may consider a change of variables $z_j = e^{-t_j/\alpha_d}$. When $\Delta E^A = \Delta E^B = \Delta E$ this integral gets significantly simplified and is evaluated to be

$$\begin{aligned} \mathcal{I}_{AB\omega_k} &= \left[\frac{e^{ik_x d}}{(\omega_k - k_x)^2} + \frac{e^{-ik_x d}}{(\omega_k + k_x)^2} \right] \\ &\quad \times \pi \alpha_d \Delta E \frac{1}{e^{2\pi\alpha_d \Delta E} - 1}. \end{aligned} \quad (87)$$

Unlike the (1 + 1) dimensional case here the integral $\mathcal{I}_{AB\omega_k}$ is not equivalent to $\mathcal{I}_{j\omega_k}$ up-to a phase factor. In (1 + 3) dimensions one also observes that the mutual information will be dependent on the parameter d

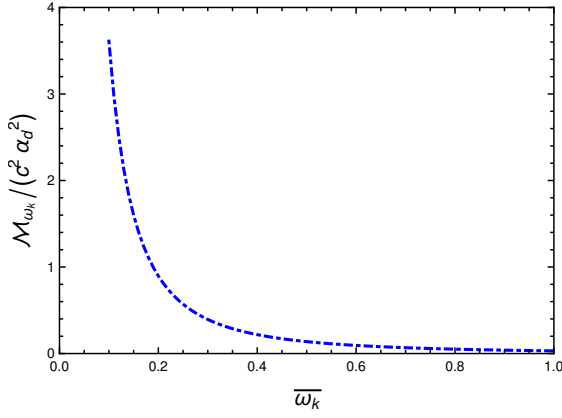


FIG. 36: The mutual information $\mathcal{M}_{\omega_k}(\rho_{AB})/(c^2 r_H^2)$ perceived by two out going null detectors in (1+3)-dimensional de Sitter spacetime corresponding to the conformal vacuum is plotted with respect to the dimensionless frequency of the field modes $\bar{\omega}_k = \alpha_d \omega_k$ for fixed transition frequency $\bar{\Delta E} = \alpha_d \Delta E = 1$, and $d/\alpha_d = 1$. Here we have also considered $\alpha_d k_x = \bar{\omega}_k/2$.

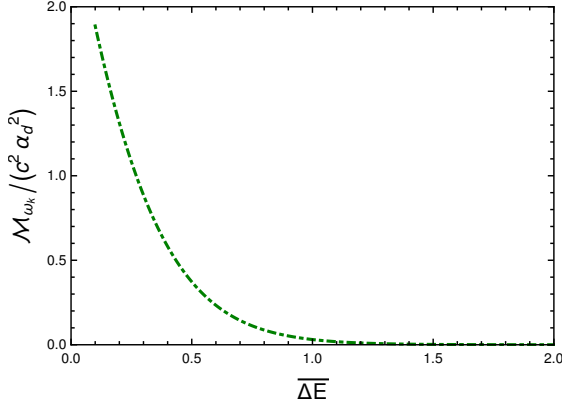


FIG. 37: The mutual information $\mathcal{M}_{\omega_k}(\rho_{AB})/(c^2 r_H^2)$ perceived by two out going null detectors in (1+3)-dimensional de Sitter spacetime corresponding to the conformal vacuum is plotted with respect to the dimensionless transition frequency $\bar{\Delta E} = \alpha_d \Delta E$ for fixed frequency of the field modes $\bar{\omega}_k = \alpha_d \omega_k = 1$, $\alpha_d k_x = \bar{\omega}_k/2$ and $d/\alpha_d = 1$.

separating two outgoing null paths. With the expression of the monopole moment operator to be $m_j(0) = |E_1^j\rangle\langle E_0^j| + |E_0^j\rangle\langle E_1^j|$ one gets the expectation values $\langle E_1^j | m_j(0) | E_0^j \rangle = 1$. In that case $P_{A\omega_k} = \mathcal{I}_{A\omega_k}$, $P_{B\omega_k} = \mathcal{I}_{B\omega_k}$, and $P_{AB\omega_k} = \mathcal{I}_{AB\omega_k}$, where

$$P_j = \int \frac{d^2 k_\perp}{(2\pi)^2 2\omega_k} \int_0^\infty dk_x P_{j\omega_k}. \quad (88)$$

When $d = 0$ and $\Delta E^A = \Delta E^A = \Delta E$ the integral $\mathcal{I}_{AB\omega_k}$ becomes same with the $\mathcal{I}_{j\omega_k}$. In that scenario one can further consider $\mathcal{I}_{A\omega_k} = \mathcal{I}_{B\omega_k} = |\mathcal{I}_{AB\omega_k}| = \mathcal{I}_{\omega_k}$. Then $P_{+\omega_k} = \mathcal{I}_{\omega_k}$ and $P_{-\omega_k} = 0$, and one can get the mutual

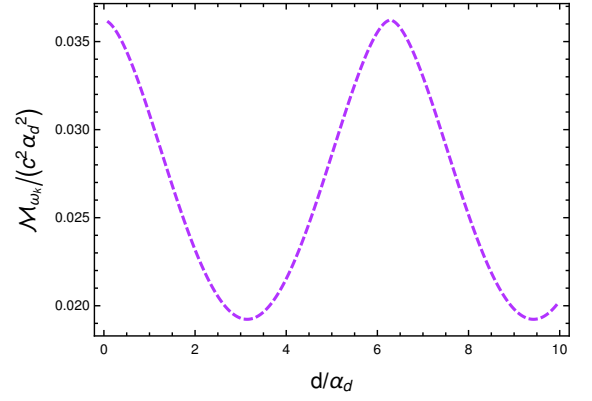


FIG. 38: The mutual information $\mathcal{M}_{\omega_k}(\rho_{AB})/(c^2 r_H^2)$ perceived by two out going null detectors in (1+3)-dimensional de Sitter spacetime corresponding to the conformal vacuum is plotted with respect to the dimensionless parameter d/α_d , for fixed transition frequency $\bar{\Delta E} = \alpha_d \Delta E = 1$, frequency of the field modes $\bar{\omega}_k = \alpha_d \omega_k = 1$, and $\alpha_d k_x = \bar{\omega}_k/2$.

information for a certain field frequency ω_k as

$$\mathcal{M}_{\omega_k}(\rho_{AB}) = c^2 2 \mathcal{I}_{\omega_k} \ln 2 + \mathcal{O}(c^4). \quad (89)$$

Then the plots corresponding to $\mathcal{M}_{\omega_k}(\rho_{AB})$ for $d = 0$ should be qualitatively same with the plots of $\mathcal{I}_{j\omega_k}$ from Fig. 26 and 29.

On the other hand, when $\Delta E^A = \Delta E^A = \Delta E$ and $d \neq 0$, one gets $P_{A\omega_k} = \mathcal{I}_{A\omega_k}$, $P_{B\omega_k} = \mathcal{I}_{B\omega_k}$, $P_{AB\omega_k} = \mathcal{I}_{AB\omega_k}$ and $P_{\pm\omega_k} = \mathcal{I}_{j\omega_k} \pm |\mathcal{I}_{AB\omega_k}|$. Using these expressions we have obtained the mutual information for $d \neq 0$. We included the plots 36 and 37 which represent the change of the mutual information with respect to $\bar{\omega}_k$ and $\bar{\Delta E}$ when $d/\alpha_d = 1$. Qualitatively these plots are not different from the ones with $d/\alpha_d = 0$. Furthermore, unlike the (1+1) dimensional de Sitter case in (1+3) dimensions, the mutual information is dependent, in fact periodically dependent, on d/α_d and this fact is graphically presented in Fig. 38.

VIII. DISCUSSION

This work investigates the entanglement harvesting with detectors in outgoing null trajectories from the conformal vacuums in de Sitter and (1+1) dimensional Schwarzschild spacetimes. In particular, we considered the momentum space representation of Green's functions to estimate the Harvesting conditions corresponding to a specific field mode frequency. We observed that entanglement harvesting is possible, and it is maximum at a particular field mode frequency in the (1+1) dimensional Schwarzschild black hole spacetime with detectors in the same outgoing null trajectory. For this specific trajectory of the same outgoing null path of the two detectors, one observes that (1+1) de Sitter spacetime does not exhibit any entanglement extraction, for the same set

of considered parameter values. It signifies that though both detectors are moving along the same outgoing null path in (1 + 1) de Sitter spacetime, there is no quantum correlation among them. We also observed that these two detectors can be classically correlated as the mutual information between them turned out to be non zero. In contrast, (1 + 3) dimensional de Sitter spacetime shows entanglement harvesting, for the two detectors in same outgoing null path. When the detectors are in different outgoing null paths, distance d apart, we observed that the concurrence becomes periodic with respect to the distance d with period and amplitude depending on the field mode frequency. It is also observed that the concurrence vanishes at periodic points in d in the (1 + 1) dimensional Schwarzschild and (1 + 3) dimensional de Sitter spacetime. However, in (1 + 1) dimensional de Sitter spacetime, it becomes zero in periodic regions of d . Therefore, as long as the concurrence is concerned one finds the (1+1) dimensional Schwarzschild and (1+3) dimensional de Sitter spacetime are qualitatively the same, providing entanglement shadow points in d .

We also observed that in (1 + 1) dimensional Schwarzschild and (1 + 3) dimensional de Sitter spacetime, regardless of whether one takes the same or different outgoing null paths, the concurrence continuously decreases with increasing detector transition energy. In (1 + 1) dimensional de Sitter spacetime and for a certain non-zero value of the distance d , one harvests entanglement in discrete ranges of the field mode frequency, see Fig. 21.

We observed that the mutual information corresponding to a specific field mode frequency is generally independent of the distance d in (1 + 1) dimensional Schwarzschild and de Sitter spacetime. In contrast, this mutual information is periodically dependent on d in (1 + 3) dimensional de Sitter background, but it never becomes zero like the concurrence. This analysis asserts that in these spacetimes, one can obtain certain outgoing null paths for the two detectors where there is no quantum communication between the two detectors. However, classical communication is still possible as perceived through mutual information.

In this analysis we intentionally refrain from making any comment on Hartle-Hawking vacuum for black hole

case. This is because we could not properly analyse the related integrals since our choices of regulators could not make the integrals convergent, both at the analytical and numerical levels. One should note that we have specifically considered the outgoing null paths for the detectors. In this regard, one could have considered the ingoing null paths as well. In particular, we have checked the case with both detectors in ingoing null paths corresponding to the Boulware, Unruh, and the Hartle-Hawking vacua. The properties of the entanglement harvesting from the Boulware vacuum, as expected, remain the same like the outgoing scenario. Whereas the ingoing-Unruh situation follows the identical outcome of outgoing-Hartle-Hawking case and therefore we refrain to comment again. Similar situation also arises for ingoing-Hartle-Hawking scenario. Finally, the de-Sitter universe also yields the identical inferences for the ingoing trajectories as the outgoing ones.

Appendix A: Evaluation of the integrals $\mathcal{I}_{\varepsilon\omega_k}^W$ and $\mathcal{I}_{\varepsilon\omega_k}^R$ in Schwarzschild black hole spacetime

1. Boulware vacuum

We introduce regulator of the form $(y_A y_B)^\epsilon e^{-\epsilon(y_A + y_B)}$ to evaluate the integral $\mathcal{I}_{\varepsilon\omega_k}^W$ from Eq. (51) corresponding to two detectors in outgoing null trajectories in an (1 + 1) dimensional Schwarzschild black hole spacetime. In particular, this integral is evaluated as

$$\begin{aligned} \mathcal{I}_{\varepsilon\omega_k}^W &= \frac{e^{id\omega_k} (4r_H^2 \omega_k^2 + 9\epsilon^2)}{r_H^2 (4\omega_k^2 - \Delta E^2) - 2i\Delta E r_H \epsilon + \epsilon^2} \\ &(\epsilon + ir_H(2\omega_k - \Delta E))^{-\epsilon + 2ir_H(\omega_k - \Delta E)} \\ &(\epsilon - ir_H(\Delta E + 2\omega_k))^{-\epsilon - 2ir_H(\Delta E + \omega_k)} \\ &\Gamma(\epsilon - 2ir_H(\omega_k - \Delta E))\Gamma(2ir_H(\omega_k + \Delta E) + \epsilon). \end{aligned} \quad (A1)$$

On the other hand, using same regulator of the form $(z_A z_B)^\epsilon e^{-\epsilon(z_A + z_B)}$ with small positive real parameter ϵ the integral $\mathcal{I}_{\varepsilon\omega_k}^R$ from Eq. (54) is evaluated as

$$\begin{aligned} \mathcal{I}_{\varepsilon\omega_k}^R &= -\frac{e^{-id\omega_k} (-1 + e^{2id\omega_k})}{(4\omega_k^2 - \Delta E^2) r_H^2 - 2i\Delta E r_H \epsilon + \epsilon^2} (ir_H(2\omega_k - \Delta E) + \epsilon)^{2ir_H(\omega_k - \Delta E) - \epsilon} (\epsilon - ir_H(2\omega_k + \Delta E))^{-2ir_H(\omega_k + \Delta E) - \epsilon} \\ &\times (4r_H^2 \omega_k^2 + 9\epsilon^2) \Gamma(\epsilon - 2ir_H(\omega_k - \Delta E))\Gamma(2ir_H(\omega_k + \Delta E) + \epsilon) \\ &+ \left[-\frac{4ie^{id\omega_k} (ir_H(2\omega_k - \Delta E) + \epsilon)^{-2(2ir_H \Delta E + \epsilon)}}{2r_H(\omega_k + \Delta E) - i\epsilon} \right. \\ &\left. \times {}_2F_1 \left(2(2ir_H \Delta E + \epsilon), 2ir_H(\omega_k + \Delta E) + \epsilon; 2ir_H(\omega_k + \Delta E) + \epsilon + 1; \frac{2r_H \omega_k + r_H \Delta E + i\epsilon}{2r_H \omega_k - r_H \Delta E - i\epsilon} \right) \right] \end{aligned}$$

$$\begin{aligned}
& + \frac{4e^{-id\omega_k}(2ir_H\Delta E + \epsilon)(\epsilon - ir_H(2\omega_k + \Delta E))^{-2(2ir_H\Delta E + \epsilon)}}{(2r_H(\omega_k - \Delta E) + i\epsilon)(r_H(2\omega_k + \Delta E) + i\epsilon)} \\
& \times {}_2F_1\left(\epsilon - 2ir_H(\omega_k - \Delta E), 4ir_H\Delta E + 2\epsilon + 1; -2ir_H(\omega_k - \Delta E) + \epsilon + 1; \frac{2r_H\omega_k - r_H\Delta E - i\epsilon}{2r_H\omega_k + r_H\Delta E + i\epsilon}\right) \\
& - \frac{4e^{-id\omega_k}(2ir_H\Delta E + \epsilon)(\epsilon - ir_H(2\omega_k + \Delta E))^{-4ir_H\Delta E - 2\epsilon - 1}}{-2ir_H(\omega_k - \Delta E) + \epsilon + 1} \\
& \times {}_2F_1\left(-2ir_H(\omega_k - \Delta E) + \epsilon + 1, 4ir_H\Delta E + 2\epsilon + 1; -2ir_H(\omega_k - \Delta E) + \epsilon + 2; \frac{2r_H\omega_k - r_H\Delta E - i\epsilon}{2r_H\omega_k + r_H\Delta E + i\epsilon}\right) \\
& - \frac{2e^{id\omega_k}(2r_H\Delta E - i\epsilon)(ir_H(2\omega_k - \Delta E) + \epsilon)^{-4ir_H\Delta E - 2(\epsilon + 1)}(4r_H\Delta E - i(2\epsilon + 1))}{2ir_H(\omega_k + \Delta E) + \epsilon + 1} \\
& \times {}_2F_1\left(2(2ir_H\Delta E + \epsilon + 1), 2ir_H(\omega_k + \Delta E) + \epsilon + 1; 2ir_H(\omega_k + \Delta E) + \epsilon + 2; \frac{2r_H\omega_k + r_H\Delta E + i\epsilon}{2r_H\omega_k - r_H\Delta E - i\epsilon}\right) \\
& - \frac{4ie^{id\omega_k}(ir_H(2\omega_k - \Delta E) + \epsilon)^{-4ir_H\Delta E - 2\epsilon - 1}(2ir_H\Delta E + \epsilon)}{2r_H(\omega_k + \Delta E) - i\epsilon} \\
& \times {}_2F_1\left(2ir_H(\omega_k + \Delta E) + \epsilon, 4ir_H\Delta E + 2\epsilon + 1; 2ir_H(\omega_k + \Delta E) + \epsilon + 1; \frac{2r_H\omega_k + r_H\Delta E + i\epsilon}{2r_H\omega_k - r_H\Delta E - i\epsilon}\right) \\
& + \frac{4e^{id\omega_k}(ir_H(2\omega_k - \Delta E) + \epsilon)^{-4ir_H\Delta E - 2\epsilon - 1}(2ir_H\Delta E + \epsilon)}{2ir_H(\omega_k + \Delta E) + \epsilon + 1} \\
& \times {}_2F_1\left(2ir_H(\omega_k + \Delta E) + \epsilon + 1, 4ir_H\Delta E + 2\epsilon + 1; 2ir_H(\omega_k + \Delta E) + \epsilon + 2; \frac{2r_H\omega_k + r_H\Delta E + i\epsilon}{2r_H\omega_k - r_H\Delta E - i\epsilon}\right) \\
& + \frac{8i(\epsilon - ir_H\Delta E)^{-4ir_H\Delta E - 2\epsilon} {}_2F_1(2ir_H\Delta E + \epsilon, 2(2ir_H\Delta E + \epsilon); 2ir_H\Delta E + \epsilon + 1; -1) \sin(d\omega_k)}{2ir_H\Delta E + \epsilon} \\
& + \frac{8i(\epsilon - ir_H\Delta E)^{-4ir_H\Delta E - 2\epsilon - 1}(2ir_H\Delta E + \epsilon) \sin(d\omega_k)}{2ir_H\Delta E + \epsilon + 1} \\
& \times {}_2F_1(2ir_H\Delta E + \epsilon + 1, 4ir_H\Delta E + 2\epsilon + 1; 2ir_H\Delta E + \epsilon + 2; -1) \\
& + \frac{4(2r_H\Delta E - i\epsilon)(\epsilon - ir_H\Delta E)^{-4ir_H\Delta E - 2\epsilon - 1}(4r_H\Delta E - i(2\epsilon + 1)) \sin(d\omega_k)}{(r_H\Delta E + i\epsilon)(2ir_H\Delta E + \epsilon + 1)} \\
& \times {}_2F_1(2ir_H\Delta E + \epsilon + 1, 2(2ir_H\Delta E + \epsilon + 1); 2ir_H\Delta E + \epsilon + 2; -1) \\
& - \frac{4e^{-id\omega_k}(\epsilon - ir_H(2\omega_k + \Delta E))^{-4ir_H\Delta E - 2\epsilon}}{\epsilon - 2ir_H(\omega_k - \Delta E)} \\
& \times {}_2F_1\left(\epsilon - 2ir_H(\omega_k - \Delta E), 2(2ir_H\Delta E + \epsilon); -2ir_H(\omega_k - \Delta E) + \epsilon + 1; \frac{2r_H\omega_k - r_H\Delta E - i\epsilon}{2r_H\omega_k + r_H\Delta E + i\epsilon}\right) \\
& - \frac{2e^{-id\omega_k}(2r_H\Delta E - i\epsilon)(\epsilon - ir_H(2\omega_k + \Delta E))^{-2(2ir_H\Delta E + \epsilon)}(4r_H\Delta E - i(2\epsilon + 1))}{(r_H(2\omega_k + \Delta E) + i\epsilon)^2(-2ir_H(\omega_k - \Delta E) + \epsilon + 1)} \\
& \times {}_2F_1\left(-2ir_H(\omega_k - \Delta E) + \epsilon + 1, 2(2ir_H\Delta E + \epsilon + 1); -2ir_H(\omega_k - \Delta E) + \epsilon + 2; \frac{2r_H\omega_k - r_H\Delta E - i\epsilon}{2r_H\omega_k + r_H\Delta E + i\epsilon}\right) \\
& - \frac{8(\epsilon - ir_H\Delta E)^{-2(2ir_H\Delta E + \epsilon)} {}_2F_1(2ir_H\Delta E + \epsilon, 4ir_H\Delta E + 2\epsilon + 1; 2ir_H\Delta E + \epsilon + 1; -1) \sin(d\omega_k)}{r_H\Delta E + i\epsilon} \Big] \Gamma(4ir_H\Delta E + 2\epsilon) \\
& + \frac{2(\epsilon - ir_H\Delta E)^{-2(2ir_H\Delta E + \epsilon)} (-8ir_H^2\Delta E^2 + 4r_H\epsilon\Delta E + 5i\epsilon^2) \Gamma(2ir_H\Delta E + \epsilon)^2 \sin(d\omega_k)}{(r_H\Delta E + i\epsilon)^2} \\
& + \frac{8(\epsilon - ir_H\Delta E)^{-2(2ir_H\Delta E + \epsilon)} \Gamma(2ir_H\Delta E + \epsilon) \Gamma(2ir_H\Delta E + \epsilon + 1) \sin(d\omega_k)}{r_H\Delta E + i\epsilon}. \tag{A2}
\end{aligned}$$

For both $\mathcal{I}_{\epsilon\omega_k}^W$ and $\mathcal{I}_{\epsilon\omega_k}^R$ we have considered the evaluation for $\Delta E^A = \Delta E^B = \Delta E$. Here the functions $\Gamma(x)$ and ${}_2F_1(x)$ respectively denote the *Gamma functions* and the

Hypergeometric functions.

2. Unruh vacuum

One can introduce regulator of the form $(y_A y_B)^\epsilon e^{-\epsilon(y_A + y_B)}$ to evaluate the integral $\mathcal{I}_{\bar{\omega}_k}^W$ from Eq. (57) corresponding to detectors in outgoing null trajectories in an (1 + 1) dimensional Schwarzschild black hole spacetime with Unruh vacuum. In particular, this integral has the same expression as provided in Eq. (A1).

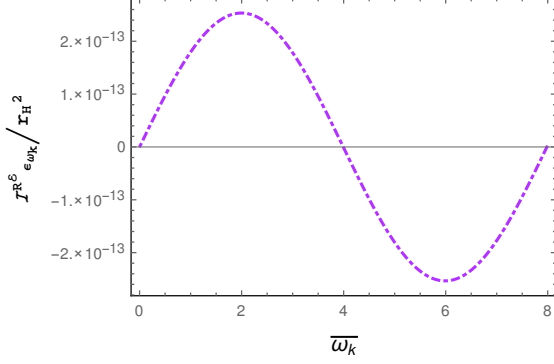


FIG. 39: The quantity $\mathcal{I}_{\bar{\omega}_k}^{R^\epsilon}$ is plotted with respect to $\bar{\omega}_k$ for fixed $d/r_H = 1$, $\Delta E = 1$.

On the other hand, utilizing the same regulator of the form $(y_A y_B)^\epsilon e^{-\epsilon(y_A + y_B)}$ one can also proceed to evaluate the integral $\mathcal{I}_{\bar{\omega}_k}^R$ from Eq. (58). In particular, one can observe that this integral is different from Eq. (53) of the Boulware case in only the last term with a factor of $-2i \sin\{\omega_k 2r_H(1 - \exp(-d/2r_H))\}$. Let us term this quantity to be $\mathcal{I}_{\bar{\omega}_k}^{R^\epsilon}$ and evaluate this integral

$$\begin{aligned} \mathcal{I}_{\bar{\omega}_k}^{R^\epsilon} &= -2i \sin\left\{\omega_k 2r_H(1 - e^{-d/2r_H})\right\} \int_{r_H}^{\infty} dr_A \frac{r_A + r_H}{r_A - r_H} \\ &\times \int_{r_H}^{r_A} dr_B \frac{r_B + r_H}{r_B - r_H} e^{i\{\Delta E^B r_B + \Delta E^A(r_A + d)\}} \\ &\times \left(\frac{r_B}{r_H} - 1\right)^{2ir_H \Delta E^B} \left(\frac{r_A}{r_H} - 1\right)^{2ir_H \Delta E^A}. \end{aligned} \quad (\text{A3})$$

This integral can be evaluated with regulator $(y_A y_B)^\epsilon e^{-\epsilon(y_A + y_B)}$ and is obtained as

$$\begin{aligned} \mathcal{I}_{\bar{\omega}_k}^{R^\epsilon} &= -2 \sin\left\{\omega_k 2r_H(1 - e^{-d/2r_H})\right\} (\epsilon - i\Delta E r_H)^{-4i\Delta E r_H - 2\epsilon - 1} \\ &\left[2 \left\{ -\frac{2(\Delta E r_H + i\epsilon) {}_2F_1(2ir_H \Delta E + \epsilon, 2(2ir_H \Delta E + \epsilon); 2ir_H \Delta E + \epsilon + 1; -1)}{\epsilon + 2i\Delta E r_H} \right. \right. \\ &- 2i {}_2F_1(2ir_H \Delta E + \epsilon, 4ir_H \Delta E + 2\epsilon + 1; 2ir_H \Delta E + \epsilon + 1; -1) \\ &+ \frac{(4i\Delta E r_H + 2\epsilon + 1)(2\Delta E r_H - i\epsilon) {}_2F_1(2ir_H \Delta E + \epsilon + 1, 2(2ir_H \Delta E + \epsilon + 1); 2ir_H \Delta E + \epsilon + 2; -1)}{(\Delta E r_H + i\epsilon)(2\Delta E r_H - i(\epsilon + 1))} \\ &\left. \left. - \frac{2i(2\Delta E r_H - i\epsilon) {}_2F_1(2ir_H \Delta E + \epsilon + 1, 4ir_H \Delta E + 2\epsilon + 1; 2ir_H \Delta E + \epsilon + 2; -1)}{2\Delta E r_H - i(\epsilon + 1)} \right\} \Gamma(4ir_H \Delta E + 2\epsilon) \right. \\ &\left. + \frac{(8\Delta E^2 r_H^2 + 4i\Delta E r_H \epsilon - 5\epsilon^2) \Gamma(2ir_H \Delta E + \epsilon)^2}{\Delta E r_H + i\epsilon} + 4i\Gamma(2ir_H \Delta E + \epsilon + 1)\Gamma(2ir_H \Delta E + \epsilon) \right]. \end{aligned} \quad (\text{A4})$$

One can numerically plot this quantity for similar parameter values for which the plots of $\mathcal{I}_{\bar{\omega}_k}^R$ are performed and observe that $\mathcal{I}_{\bar{\omega}_k}^{R^\epsilon}$ is many order lower, see. Fig. 39.

Appendix B: Heaviside step function corresponding to the Unruh modes

The Kruskal null coordinates (V, U) are related to the null coordinates (v, u) by the relation $V = 2r_H e^{v/2r_H}$ and $U = -2r_H e^{-u/2r_H}$. Whereas these coordinates (v, u) are again related to the Schwarzschild time and the

tortoise coordinates as $v = t_s + r_*$ and $u = t_s - r_*$. We have already stated that while dealing with modes represented in terms of the Kruskal coordinates one should consider the Kruskal time $T_K = (U + V)/2$. This time is represented in terms of the Schwarzschild time and the tortoise coordinates as $T_K = 2r_H e^{r_*/2r_H} \sinh(t_s/2r_H)$. We have considered that Alice and Bob denoted respectively by the detectors A and B are both moving along outgoing null trajectories. However, for Alice the outgoing null path is $t_{sA} - r_{*A} = d$, while for Bob the path is $t_{sB} - r_{*B} = 0$. With these conditions let us search for the situation when the Heaviside step function $\theta(T_{K_A} - T_{K_B})$

will be non zero.

For the above mentioned Heaviside step function to be non zero one must have $T_{K_A} \geq T_{K_B}$. In terms of the Schwarzschild time and the tortoise coordinate and using the appropriate prescription of the null paths for the detectors A and B this condition becomes

$$e^{(2r_{*A}+d)/2r_H} - e^{r_{*B}/r_H} \geq e^{-d/2r_H} - 1. \quad (\text{B1})$$

Here we have considered d to be positive and real. In that case the maximum value of the right hand side of the above inequality is zero and therefore the above will be automatically satisfied if one has

$$e^{(2r_{*A}+d)/2r_H} - e^{r_{*B}/r_H} \geq 0. \quad (\text{B2})$$

This can be re-expressed as $e^{(r_{*A}-r_{*B})/r_H} \geq e^{-(d/2r_H)}$. Now again as $0 \leq e^{-(d/2r_H)} \leq 1$, the required condition will be satisfied if one has

$$e^{(r_{*A}-r_{*B})/r_H} \geq 1. \quad (\text{B3})$$

This basically implies that one must have $r_{*A} \geq r_{*B}$ or

$r_A \geq r_B$. Note that this very condition has been considered in our main analysis.

Appendix C: Evaluation of the integrals $\mathcal{I}_{\varepsilon\omega_k}^W$ and $\mathcal{I}_{\varepsilon\omega_k}^R$ in de Sitter spacetime

1. (1 + 1) dimensions

With the introduction of regulator of the form $(z_A z_B)^\epsilon e^{-\epsilon(z_A+z_B)}$ the integral $\mathcal{I}_{\varepsilon\omega_k}^W$ from Eq. (66) corresponding to two detectors in outgoing null trajectories in an (1 + 1) dimensional de Sitter spacetime can be evaluated to be

$$\mathcal{I}_{\varepsilon\omega_k}^W = e^{-id\omega_k} \Gamma(\epsilon - i\alpha_d \Delta E)^2 (\epsilon - 2i\alpha_d \omega_k)^{-\epsilon+i\alpha_d \Delta E} \times (\epsilon + 2i\alpha_d \omega_k)^{-\epsilon+i\alpha_d \Delta E}. \quad (\text{C1})$$

On the other hand, using same regulator of the form $(z_A z_B)^\epsilon e^{-\epsilon(z_A+z_B)}$ with small positive real parameter ϵ the integral $\mathcal{I}_{\varepsilon\omega_k}^R$ from Eq. (67) is evaluated as

$$\begin{aligned} \mathcal{I}_{\varepsilon\omega_k}^R &= \Gamma(\epsilon - i\alpha_d \Delta E) \left[\Gamma(2\epsilon - 2i\alpha_d \Delta E) \left\{ e^{id\omega_k} (\epsilon + 2i\alpha_d \omega_k)^{-2\epsilon+2i\alpha_d \Delta E} \right. \right. \\ &\quad \left. \left. {}_2\tilde{F}_1 \left(\epsilon - i\alpha_d \Delta E, 2(\epsilon - i\alpha_d \Delta E); -i\alpha_d \Delta E + \epsilon + 1; \frac{4i\omega_k \alpha_d}{2i\omega_k \alpha_d + \epsilon} - 1 \right) - e^{-id\omega_k} (\epsilon - 2i\alpha_d \omega_k)^{-2\epsilon+2i\alpha_d \Delta E} \right. \right. \\ &\quad \left. \left. {}_2\tilde{F}_1 \left(\epsilon - i\alpha_d \Delta E, 2(\epsilon - i\alpha_d \Delta E); -i\alpha_d \Delta E + \epsilon + 1; \frac{4\omega_k \alpha_d}{2\omega_k \alpha_d + i\epsilon} - 1 \right) \right\} - i\epsilon^{-2\epsilon+2i\alpha_d \Delta E} \sin(d\omega_k) \Gamma(\epsilon - i\alpha_d \Delta E) \right]. \end{aligned} \quad (\text{C2})$$

For both $\mathcal{I}_{\varepsilon\omega_k}^W$ and $\mathcal{I}_{\varepsilon\omega_k}^R$ we have considered the evaluation for $\Delta E^A = \Delta E^B = \Delta E$. Here the functions $\Gamma(x)$ and ${}_2\tilde{F}_1(x)$ respectively denote the *Gamma functions* and the *regularized Hypergeometric functions*.

2. (1 + 3) dimensions

With the introduction of regulator of the form $(z_A z_B)^\epsilon e^{-\epsilon(z_A+z_B)}$ the integral $\mathcal{I}_{\varepsilon\omega_k}^W$ from Eq. (74) corresponding to two detectors in outgoing null trajectories in an (1 + 3) dimensional de Sitter spacetime can be eval-

uated to be

$$\begin{aligned} \mathcal{I}_{\varepsilon\omega_k}^W &= e^{-id\omega_k} \Gamma(-i\alpha_d \Delta E + \epsilon + 1)^2 \\ &\quad \times (\epsilon - i\alpha_d (k_x + \omega_k))^{i\alpha_d \Delta E - \epsilon - 1} \\ &\quad (\epsilon + i\alpha_d (k_x + \omega_k))^{i\alpha_d \Delta E - \epsilon - 1} + e^{id\omega_k} \Gamma(-i\alpha_d \Delta E + \epsilon + 1)^2 \\ &\quad (\epsilon - i\alpha_d (k_x - \omega_k))^{i\alpha_d \Delta E - \epsilon - 1} (i\alpha_d k_x - i\alpha_d \omega_k + \epsilon)^{i\alpha_d \Delta E - \epsilon - 1}. \end{aligned} \quad (\text{C3})$$

On the other hand, using same regulator of the form $(z_A z_B)^\epsilon e^{-\epsilon(z_A+z_B)}$ with small positive real parameter ϵ the integral $\mathcal{I}_{\varepsilon\omega_k}^R$ from Eq. (75) is evaluated as

$$\begin{aligned} \mathcal{I}_{\varepsilon\omega_k}^R &= \frac{e^{-idk_x}}{-i\alpha_d \Delta E + \epsilon + 1} \Gamma(-2i\alpha_d \Delta E + 2\epsilon + 2) \left[(\epsilon - i\alpha_d (k_x - \omega_k))^{-2(\epsilon+1)+2i\alpha_d \Delta E} \right. \\ &\quad \left. \times {}_2F_1 \left(-i\alpha_d \Delta E + \epsilon + 1, -2i\alpha_d \Delta E + 2\epsilon + 2; -i\alpha_d \Delta E + \epsilon + 2; \frac{k_x \alpha_d - \omega_k \alpha_d - i\epsilon}{k_x \alpha_d - \omega_k \alpha_d + i\epsilon} \right) \right] \end{aligned}$$

$$\begin{aligned}
& -e^{2idk_x}(\epsilon + i\alpha_d(k_x - \omega_k))^{-2(\epsilon+1)+2i\alpha_d\Delta E} \\
& \times {}_2F_1\left(-i\alpha_d\Delta E + \epsilon + 1, -2i\alpha_d\Delta E + 2\epsilon + 2; -i\alpha_d\Delta E + \epsilon + 2; \frac{k_x\alpha_d - \omega_k\alpha_d + i\epsilon}{k_x\alpha_d - \omega_k\alpha_d - i\epsilon}\right) \\
& + e^{-idk_x}\Gamma(-i\alpha_d\Delta E + \epsilon + 1)\Gamma(-2i\alpha_d\Delta E + 2\epsilon + 2)\left[e^{2idk_x}(\epsilon + i\alpha_d(k_x + \omega_k))^{-2(\epsilon+1)+2i\alpha_d\Delta E}\right. \\
& \times {}_2\tilde{F}_1\left(-i\alpha_d\Delta E + \epsilon + 1, 2(-i\alpha_d\Delta E + \epsilon + 1); -i\alpha_d\Delta E + \epsilon + 2; \frac{(k_x + \omega_k)\alpha_d + i\epsilon}{(k_x + \omega_k)\alpha_d - i\epsilon}\right) \\
& \left. - (\epsilon - i\alpha_d(k_x + \omega_k))^{-2(\epsilon+1)+2i\alpha_d\Delta E}\right. \\
& \left. \times {}_2\tilde{F}_1\left(-i\alpha_d\Delta E + \epsilon + 1, 2(-i\alpha_d\Delta E + \epsilon + 1); -i\alpha_d\Delta E + \epsilon + 2; \frac{(k_x + \omega_k)\alpha_d - i\epsilon}{(k_x + \omega_k)\alpha_d + i\epsilon}\right)\right]. \quad (C4)
\end{aligned}$$

Here also we have considered the specific scenario $\Delta E^A = \Delta E^B = \Delta E$ for evaluating both $\mathcal{I}_{\epsilon\omega_k}^W$ and $\mathcal{I}_{\epsilon\omega_k}^R$, and the functions $\Gamma(x)$, ${}_2F_1(x)$ and ${}_2\tilde{F}_1(x)$ respectively denote the *Gamma functions*, the *Hypergeometric functions*, and the *regularized Hypergeometric functions*.

Acknowledgments

DB and SB would like to thank the Indian Institute of Technology Guwahati (IIT Guwahati) for supporting this

work through Doctoral and Post-Doctoral Fellowships. The research of BRM is partially supported by a START-UP RESEARCH GRANT (No. SG/PHY/P/BRM/01) from the Indian Institute of Technology Guwahati, India.

-
- [1] B. Reznik, *Found. Phys.* **33**, 167 (2003), arXiv:quant-ph/0212044.
- [2] S.-Y. Lin and B. Hu, *Phys. Rev. D* **81**, 045019 (2010), arXiv:0910.5858.
- [3] J. L. Ball, I. Fuentes-Schuller, and F. P. Schuller, *Phys. Lett. A* **359**, 550 (2006), arXiv:quant-ph/0506113.
- [4] M. Cliche and A. Kempf, *Phys. Rev. A* **81**, 012330 (2010), arXiv:0908.3144.
- [5] E. Martin-Martinez and N. C. Menicucci, *Class. Quant. Grav.* **29**, 224003 (2012), arXiv:1204.4918.
- [6] G. Salton, R. B. Mann, and N. C. Menicucci, *New J. Phys.* **17**, 035001 (2015), arXiv:1408.1395.
- [7] E. Martin-Martinez, A. R. H. Smith, and D. R. Terno, *Phys. Rev. D* **93**, 044001 (2016), arXiv:1507.02688.
- [8] H. Cai and Z. Ren, *Sci. Rep.* **8**, 11802 (2018).
- [9] G. Menezes, *Phys. Rev.* **D97**, 085021 (2018), arXiv:1712.07151.
- [10] G. Menezes, N. Svaiter, and C. Zarro, *Phys. Rev. A* **96**, 062119 (2017), arXiv:1709.08702.
- [11] W. Zhou and H. Yu, *Phys. Rev. D* **96**, 045018 (2017).
- [12] F. Benatti and R. Floreanini, *Phys. Rev. A* **70**, 012112 (2004).
- [13] Y. Pan and B. Zhang, *Phys. Rev. A* **101**, 062111 (2020), arXiv:2009.05179.
- [14] G. Menezes, *Phys. Rev.* **D94**, 105008 (2016), arXiv:1512.03636.
- [15] W. Cong, C. Qian, M. R. R. Good, and R. B. Mann, *JHEP* **10**, 067 (2020), arXiv:2006.01720.
- [16] P. Chowdhury and B. R. Majhi (2021), arXiv:2110.11260.
- [17] G. R. Kane and B. R. Majhi, *Phys. Rev. D* **104**, 041701 (2021), arXiv:2105.11709.
- [18] D. Barman and B. R. Majhi (2021), arXiv:2111.00711.
- [19] I. Fuentes-Schuller and R. B. Mann, *Phys. Rev. Lett.* **95**, 120404 (2005), arXiv:quant-ph/0410172.
- [20] J. Hu and H. Yu, *Phys. Rev. A* **91**, 012327 (2015), arXiv:1501.03321.
- [21] S. Barman and B. R. Majhi, *JHEP* **03**, 245 (2021), arXiv:2101.08186.
- [22] S. J. Summers and R. Werner, *Physics Letters A* **110**, 257 (1985), ISSN 0375-9601.
- [23] S. J. Summers and R. Werner, *Journal of Mathematical Physics* **28**, 2440 (1987), <https://doi.org/10.1063/1.527733>.
- [24] A. Valentini, *Physics Letters A* **153**, 321 (1991), ISSN 0375-9601.
- [25] B. Reznik, A. Retzker, and J. Silman, *Phys. Rev. A* **71**, 042104 (2005), arXiv:quant-ph/0310058.
- [26] L. J. Henderson, R. A. Hennigar, R. B. Mann, A. R. Smith, and J. Zhang, *Class. Quant. Grav.* **35**, 21LT02 (2018), arXiv:1712.10018.
- [27] L. J. Henderson and N. C. Menicucci, *Phys. Rev. D* **102**, 125026 (2020), arXiv:2005.05330.
- [28] N. Stritzelberger, L. J. Henderson, V. Baccetti, N. C. Menicucci, and A. Kempf (2020), arXiv:2006.11291.
- [29] M. Hotta, *Phys. Rev. D* **78**, 045006 (2008), arXiv:0803.2272.
- [30] M. Hotta, *Journal of the Physical Society of Japan* **78**, 034001 (2009).

- [31] M. Frey, K. Funo, and M. Hotta, *Phys. Rev. E* **90**, 012127 (2014).
- [32] G. L. Ver Steeg and N. C. Menicucci, *Phys. Rev. D* **79**, 044027 (2009), arXiv:0711.3066.
- [33] A. Pozas-Kerstjens and E. Martín-Martínez, *Phys. Rev. D* **92**, 064042 (2015), arXiv:1506.03081.
- [34] S. Kukita and Y. Nambu, *Entropy* **19**, 449 (2017), arXiv:1708.01359.
- [35] A. Pozas-Kerstjens and E. Martín-Martínez, *Phys. Rev. D* **94**, 064074 (2016), arXiv:1605.07180.
- [36] E. Martín-Martínez, E. G. Brown, W. Donnelly, and A. Kempf, *Phys. Rev. A* **88**, 052310 (2013), arXiv:1309.1090.
- [37] K. Lorek, D. Pecak, E. G. Brown, and A. Dragan, *Phys. Rev. A* **90**, 032316 (2014), arXiv:1405.4449.
- [38] E. G. Brown, W. Donnelly, A. Kempf, R. B. Mann, E. Martín-Martínez, and N. C. Menicucci, *New J. Phys.* **16**, 105020 (2014), arXiv:1407.0071.
- [39] A. Sachs, R. B. Mann, and E. Martín-Martínez, *Phys. Rev. D* **96**, 085012 (2017), arXiv:1704.08263.
- [40] J. Trevison, K. Yamaguchi, and M. Hotta, *J. Phys. A* **52**, 125402 (2019), arXiv:1807.03467.
- [41] T. Li, B. Zhang, and L. You, *Phys. Rev. D* **97**, 045005 (2018), arXiv:1802.07886.
- [42] A. Peres, *Phys. Rev. Lett.* **77**, 1413 (1996), arXiv:quant-ph/9604005.
- [43] M. Horodecki, P. Horodecki, and R. Horodecki, *Phys. Lett. A* **223**, 1 (1996), arXiv:quant-ph/9605038.
- [44] J.-I. Koga, G. Kimura, and K. Maeda, *Phys. Rev. A* **97**, 062338 (2018), arXiv:1804.01183.
- [45] K. K. Ng, R. B. Mann, and E. Martín-Martínez, *Phys. Rev. D* **97**, 125011 (2018), arXiv:1805.01096.
- [46] J.-i. Koga, K. Maeda, and G. Kimura, *Phys. Rev. D* **100**, 065013 (2019), arXiv:1906.02843.
- [47] E. Tjoa and R. B. Mann, *JHEP* **08**, 155 (2020), arXiv:2007.02955.
- [48] J. Foo, R. B. Mann, and M. Zych, *Phys. Rev. D* **103**, 065013 (2021), arXiv:2101.01912.
- [49] K. Gallock-Yoshimura, E. Tjoa, and R. B. Mann, *Phys. Rev. D* **104**, 025001 (2021), 2102.09573.
- [50] L. J. Henderson, R. A. Hennigar, R. B. Mann, A. R. H. Smith, and J. Zhang, *JHEP* **05**, 178 (2019), arXiv:1809.06862.
- [51] K. K. Ng, R. B. Mann, and E. Martín-Martínez, *Phys. Rev. D* **98**, 125005 (2018), arXiv:1809.06878.
- [52] W. Cong, E. Tjoa, and R. B. Mann, *JHEP* **06**, 021 (2019), [Erratum: *JHEP* **07**, 051 (2019)], arXiv:1810.07359.
- [53] D. Barman, S. Barman, and B. R. Majhi, *JHEP* **07**, 124 (2021), arXiv:2104.11269.
- [54] M. P. G. Robbins, L. J. Henderson, and R. B. Mann (2020), arXiv:2010.14517.
- [55] N. D. Birrell and P. C. W. Davies, *Quantum fields in curved space*, Cambridge Monographs on Mathematical Physics (Cambridge University Press, 1984).
- [56] A. Das, S. Dalui, C. Chowdhury, and B. R. Majhi, *Phys. Rev. D* **100**, 085002 (2019), arXiv:1902.03735.
- [57] M. O. Scully, S. Fulling, D. Lee, D. N. Page, W. Schleich, and A. Svidzinsky, *Proc. Nat. Acad. Sci.* **115**, 8131 (2018), arXiv:1709.00481.
- [58] K. Chakraborty and B. R. Majhi, *Phys. Rev. D* **100**, 045004 (2019), arXiv:1905.10554.
- [59] S. Dalui and B. R. Majhi, *Phys. Rev. D* **102**, 124047 (2020), arXiv:2007.14312.
- [60] S. W. Hawking, *Comm. Math. Phys.* **43**, 199 (1975).
- [61] W. Unruh, *Phys. Rev. D* **14**, 870 (1976).
- [62] W. G. Unruh and R. M. Wald, *Phys. Rev. D* **29**, 1047 (1984).
- [63] S. Hawking and W. Israel, *General Relativity: an Einstein Centenary Survey* (2010).
- [64] K. Zyczkowski, P. Horodecki, A. Sanpera, and M. Lewenstein, *Phys. Rev. A* **58**, 883 (1998), arXiv:quant-ph/9804024.
- [65] G. Vidal and R. F. Werner, *Phys. Rev. A* **65**, 032314 (2002), arXiv:quant-ph/0102117.
- [66] J. Eisert and M. B. Plenio, *J. Mod. Opt.* **46**, 145 (1999), arXiv:quant-ph/9807034.
- [67] I. Devetak and A. Winter, *Proceedings of the Royal Society A: Mathematical, Physical and Engineering Sciences* **461**, 207–235 (2005), ISSN 1471-2946.
- [68] C. H. Bennett, D. P. DiVincenzo, J. A. Smolin, and W. K. Wootters, *Phys. Rev. A* **54**, 3824 (1996), arXiv:quant-ph/9604024.
- [69] S. Hill and W. K. Wootters, *Phys. Rev. Lett.* **78**, 5022 (1997), arXiv:quant-ph/9703041.
- [70] W. K. Wootters, *Phys. Rev. Lett.* **80**, 2245 (1998), arXiv:quant-ph/9709029.
- [71] P. Simidzija and E. Martín-Martínez, *Phys. Rev. D* **98**, 085007 (2018), arXiv:1809.05547.
- [72] D. Grumiller, W. Kummer, and D. V. Vassilevich, *Phys. Rept.* **369**, 327 (2002), hep-th/0204253.
- [73] B. A. Juárez-Aubry and J. Louko, *JHEP* **05**, 140 (2018), arXiv:1804.01228.
- [74] L. Hodgkinson, *Particle detectors in curved spacetime quantum field theory* (2013), arXiv:1309.7281.